DEVELOPMENT OF DIAGNOSTIC ALGORITHMS FOR AIR BRAKES IN TRUCKS

A Dissertation

by

SANDEEP DHAR

Submitted to the Office of Graduate Studies of
Texas A&M University
in partial fulfillment of the requirements for the degree of

DOCTOR OF PHILOSOPHY

August 2010

Major Subject: Mechanical Engineering

DEVELOPMENT OF DIAGNOSTIC ALGORITHMS FOR AIR BRAKES IN TRUCKS

A Dissertation

by

SANDEEP DHAR

Submitted to the Office of Graduate Studies of
Texas A&M University
in partial fulfillment of the requirements for the degree of

DOCTOR OF PHILOSOPHY

Approved by:

Co-Chairs of Committee,	Swaroop Darbha
	K.R. Rajagopal
Committee Members,	Reza Langari
	Wei Zhan
Head of Department,	Dennis O'Neal

August 2010

Major Subject: Mechanical Engineering

ABSTRACT

Development of Diagnostic Algorithms for Air Brakes in Trucks. (August 2010)

Sandeep Dhar, B.E., University of Mumbai;

M. Tech., Indian Institute of Technology Bombay

Co–Chairs of Advisory Committee: Dr. Swaroop Darbha
Dr. K.R. Rajagopal

In this dissertation, we focus on development of algorithms for estimating the severity of air leakage and for predicting the out-of-adjustment of pushrod in an air brake system of heavy commercial vehicles. The leakage of air from the brake system causes a reduction in the steady-state pressure in the brake chamber and an increase in the lag of the braking pressure response thereby increasing the stopping distance of the vehicle. Currently a presence of leak in the system is detected for the severities of leak that cause the reservoir pressure to drop below a threshold, such as, the leakage of compressed air due to rupture of the reservoir or of the hoses carrying the compressed air. The leakage of air is also possible due to several other reasons such as, cracks in the hoses, loose couplings between the hoses etc. The severities of leak, corresponding to such situations, do not lead to the reservoir pressure drop below the threshold; therefore, their presence remains undetected. For the detection and estimation of such severities of leak, a diagnostic scheme has been given and is based on a model developed for the mass flow rate of the leakage of air from the air brake system.

Out-of-adjustment of the pushrod is the extension of pushrod beyond a predefined value and for safety concerns, an extension beyond this value is not desired.

Currently no warning system is available for monitoring the out-of-adjustment of pushrod, except, during the safety inspection. Inspection of the pushrod for out-of-adjustment is the most labor-intensive and time consuming task during a typical safety inspection procedure. For efficient and continuous monitoring of the pushrod for out-of-adjustment, a diagnostic algorithm for estimating the steady-state pushrod stroke has been developed. The scheme is expected to expedite the inspection process for the out-of-adjustment of pushrod. Experimental data from the air brake test setup at Texas A&M University has been used for corroborating both the models.

Also, the problem of parameter estimation of sequential hybrid systems such as the air brake system, has been addressed. The "hybrid" nature of the air brake system stems from the system being in different modes corresponding to different values of the displacement of the pushrod and is a result of different spring compliances associated with the pushrod in different ranges of its displacement. The air brake system is "sequential" in the sense that as the pressure increases, the displacement of the pushrod increases and there is a distinct sequence of modes that the system will transition through and upon a reduction in pressure, the sequence of modes is revisited in the reverse order. The mode to mode transition of the air brake system is governed by the parameters, such as, the clearance between the brake pad and the brake drum. The problem of estimation, that has been addressed, is as follows: Suppose the pressure in the air brake system were to be measured and that the motion of the pushrod is not measured. Is it possible to estimate the final displacement of the pushrod *without knowing the parameters*, such as the clearance, that govern the system to transition from one mode to another?

To My Parents and My Teachers

ACKNOWLEDGMENTS

"The roots of education are bitter, but the fruit is sweet". —Aristotle

The journey in the pursuit of knowledge is guided by a few individuals and without their support the journey remains incomplete. I would like to extend my sincerest gratitude to all those individuals responsible for the completion my journey.

My greatest appreciation goes to my advisors, Professor Darbha Swaroop and Professor K. R. Rajagopal, for their endless patience and guidance par-excellence. They have been a constant source of inspiration, encouragement and have greatly influenced my attitude towards learning. I consider myself fortunate to have worked under their supervision as I have learned a lot from them, both academically and otherwise. For this, I am and always will be, indebted.

With great pleasure I extend my gratitude to Professor Reza Langari and Professor Wei Zhan for kindly agreeing to be the members of my dissertation advisory committee. I thank them all for their suggestions that helped enhance the quality of this work. I would like to thank Waqar Malik, Akhilesh Rallabandi, Sai Krishna Yadlapalli and Gaurav Aggarwal for their help regarding my research work. I would like to specially thank Ramarathnam Srivatsan for the help extended during experimentation and for the valuable suggestions regarding my work and in general.

I would like to thank all my friends at Texas A&M University specially Sayak, Sameer, Ankur, Vivek and Abhishek for being wonderful friends and roommates during my stay in College Station. I thank the administrative staff in the Department of Mechanical Engineering and the Department of Electrical and Computer Engineering for their help and assistance. Finally, I would like to extend my deepest gratitude, respect and love to my parents for their relentless support, selfless love and belief within me and for their unending patience during all these years.

TABLE OF CONTENTS

CHAPTER Page

I INTRODUCTION 1

A. Background 2
1. Leak 3
2. The out-of-adjustment of pushrod 4
B. Motivation for the diagnostic schemes 7
C. Model based diagnostic system for air brakes 9
D. Air brake system - a "sequential" hybrid system 10
E. Objectives of the dissertation 12
F. Organization of this dissertation 12

II AIR BRAKE SYSTEM 14

A. Air brake system in modern commercial vehicle 14
B. The experimental setup 21

III DETECTION OF AIR LEAKAGE AND MODEL BASED ESTIMATION OF ITS SEVERITY 26

A. Existing models for a *"leak-free"* air brake system 26
1. A mode dependent model for air brake system with the driver's input 27
B. A model for the mass flow rate of leaking air 32
1. Parameter of the mass flow rate model and its estimation 33
C. "Leak" model and its corroboration 35
D. A look-up table based diagnostic scheme for leak 36

IV ESTIMATION OF THE STEADY-STATE STROKE OF PUSHROD 41

A. Existing schemes for estimation of the steady-state stroke of pushrod 41
B. Energy based pushrod stroke estimation for a single brake chamber 43
1. Treadle valve entry pressure and its effect on pushrod stroke estimation 47

CHAPTER Page

C. Steady-state pushrod stroke estimate for the test setup configuration with two brake chambers 47
1. Pressure transients in the delivery of the primary circuit 50
2. Pushrod stroke estimates for the front and the rear brake chambers 52

V ESTIMATION OF PARAMETERS OF A CLASS OF HYBRID SYSTEMS 57

A. The problem of parameter estimation 57
B. An approach to solve the problem of parameter estimation 58
C. Problem formulation 59
D. Estimation scheme 61
E. Illustrative examples 62
1. Estimation of the parameters of the hybrid system . . 65
2. Estimator design for a mechanical hybrid system . . . 69
3. Mode detection 73
F. Experimental corroboration of the estimation scheme . . . 77
G. Problem formulation with parametric uncertainty 77
1. Estimation scheme with parametric uncertainty 78
2. Parameter adaptation law 79
3. Adaptive estimation of A_p 80

VI CONCLUSIONS AND FUTURE SCOPE 84

A. Potential impact of the work 85
B. Scope of future work 86

REFERENCES 88

APPENDIX A 94

APPENDIX B 95

APPENDIX C 97

VITA 98

LIST OF TABLES

TABLE		Page
I	Details of the components used in the test setup at Texas A&M University	25
II	Nomenclature of parameters used in the governing equations [33], [36]	30
III	Leak mass flow rates for a full brake application at different supply pressures	35
IV	Pushrod stroke estimates for various supply pressures	46
V	Nomenclature of parameters/variables [33],[46], [47]	52
VI	Pushrod stroke estimates for 90 psi supply for front and rear brake chambers	56
VII	Nomenclature of parameters/variables used	63

LIST OF FIGURES

FIGURE		Page
1	Effects of leak on brake chamber pressure transients	4
2	Experimentally determined characteristics of pushrod force versus stroke [5]	6
3	Pushrod extension for different clearances and supply pressures	6
4	Modes of operation of the air brake system [19]	11
5	A simplified layout of air brake system for a tractor	15
6	S-cam foundation brake	16
7	Brake chamber	17
8	Treadle valve	18
9	Relay valve assembly	19
10	Layout of a slack adjuster	20
11	A layout of a brake drum	21
12	Experimental setup at Texas A&M University	22
13	A schematic of the experimental facility	22
14	A schematic of the experimental facility for leak test	23
15	Flow Control Valve	24
16	Modes of operation of the air brake system [19]	27
17	Pressure transients in a brake chamber during various modes of operation	28

FIGURE Page

18 A comparative plot showing the pressure predicted by the leak-free model and the measured pressure 31

19 Measured mass flow rate of leaking air for various supply pressures . 33

20 A comparative plot of "leak-free" model and the "leak" model 36

21 Estimated steady-state brake chamber pressure for 90 psi (722 kPa) supply and for 2 turns of FCV 37

22 Estimated steady-state brake chamber pressure for 80 (653 kPa) psi supply and for 2 turns of FCV 38

23 Estimated steady-state brake chamber pressure for 70 psi (584 kPa) supply and for 1/4 turns of FCV 39

24 Pushrod stroke vs. brake chamber pressure for a given clearance . . . 42

25 Pushrod stroke vs. brake chamber pressure for different clearances . . 43

26 Test setup configuration for pushrod stroke estimation - single brake chamber 44

27 Entry pressure in the treadle valve's primary circuit during braking . 48

28 Estimates of brake chamber energy without and with considering the drop in the entry pressure 49

29 Schematic for two chamber configuration of the test setup 50

30 Volume change in the primary circuit 51

31 Estimate of E_b for the front and the rear brake chamber using measured primary circuit pressure 53

32 Estimate of E_b for the front and the rear brake chamber using the predicted primary circuit pressure 54

33 Simulated response of the hybrid system 64

34 Steady-state estimate of z_1 of the pneumatic hybrid system with massless piston 67

FIGURE Page

35 Steady-state estimates of z_1 and z_2 of the pneumatic hybrid system . 70

36 (a) Mechanical hybrid system, (b) non-hybrid counterpart 70

37 Simulated response of the mechanical hybrid system 71

38 Steady-state estimates of z and z_v of the mechanical hybrid system . 74

39 Mode detection for system (5.8) 75

40 Pushrod stroke ($z_{1\,bc}(T) = 0.051\ mm$) for "type 20" brake chamber estimated using the scheme 76

41 Pushrod stroke ($z_{1\,bc}(T) = 0.061\ mm$) for "type 30" brake chamber estimated using the scheme 76

42 Steady-state estimate of z_1 and of A_p 82

43 Pushrod stroke estimates for $z_{1\,bc}(T) \approx 79\ mm,\ 55\ mm,\ 65\ mm$, for rear brake chamber ("type 30") and corresponding estimated area A_p 83

44 Calibration curve for the velocity transducer 94

CHAPTER I

INTRODUCTION

Commercial vehicles such as buses, trucks and tractor-trailers transport 23% of the total freight in the United States [1]. Every year, around 25 million childern commute through buses as one of the means of public transport [1]. The U.S. Department of Transportation reported around 9 million commercial vehicles in the United States in 2006 [1]. With the movement of such a large quantity of goods and the number of people, ensuring proper functioning of the brake system of these vehicles is important. Approximately 85% of the commercial vehicles are equipped with an air brake system with drum type brake assembly, as their primary braking device [1], [2]. In the fiscal year 2008-2009, 39.29%[1] of the total number of vehicles inspected were reported to be out-of-service. Some of the major causes for a commercial vehicle to be out-of-service have been attributed to driver fatugue, road condition, faults in the mechanical and pneumatic subsystems of the air brake system. The two major faults that are related to the pneumatic subsystem of an air brake system and seriously affect its performance are:

1. Leakage of compressed air in the brake lines: This fault leads to a reduction in the mass flow rate of air entering the brake chamber. Consequently, there is an increased lag in the braking and a reduced steady-state pressure in the brake chamber.

2. Out-of-Adjustment of the pushrod: The pushrod is connected to the piston in

---

The journal model is *IEEE Transactions on Automatic Control.*

[1]Data Source: FMCSA Motor Carrier Management Information System (MCMIS) data snapshot

the brake chamber and is a vital component in the mechanism that translates the motion of the piston into braking action. A pushrod is said to be out-of-adjustment if its displacement/stroke exceeds a predefined limit. An increase in the stroke of the pushrod increases the lag and delay in the response of brake pressure. In some cases, there can be a significant drop in the force transmitted via pushrod to the brake pads and the drum.

The focus of dissertation is on the development of diagnostic algorithms for the two major faults listed above. Specifically, the following algorithms are the focus of this dissertation:

1. Detection and estimation of severity of the leakage of air from the air brake system.

2. Estimation of the extent of out-of-adjustment of the pushrod.

A. Background

Heavy commercial vehicles have a Gross Vehicle Weight Rating[2] (GVWR) of 14,000 kg (31,000 lb) or more. Tractor-trailer combinations, trucks and buses are classified under heavy commercial vehicles and are one of the primary carriers of people and goods within the USA and around the world. These vehicles require large braking force, unlike small vehicles, where hydraulic brakes are used to generate the required braking force. Hydraulic brakes generate the braking force by amplifying the force exerted on the brake pedal by the driver, which is then transmitted to the brake pads via an incompressible braking fluid[3]. If one were to use hydraulic brakes in a

[2]Maximum recommended weight for a vehicle, including: the weight of the vehicle itself, fuel and other fluids, passengers and all cargo.

[3]Here, by a fluid, we mean the braking liquid which is also referred as *brake fluid*. This is a specially manufactured liquid; hence, it is not as readily available as air.

commercial vehicle, the braking force required to operate the vehicle necessitates the use of large size brake chambers or high pressures or both. Usually, the space available for mounting the brake chambers is limited by the size of the commercial vehicle and therefore, large size brake chambers are not preferred. Also, the loss of braking fluid in the hydraulic brake cannot be replenished immediately and such a situation is extremely dangerous for the commercial vehicle and the other vehicles in the vicinity. Air brake system overcomes these difficulties by using compressed air as the working fluid. Air can be easily compressed to high pressures which allows for the use of smaller brake chambers to generate the desired braking force. Also, air is abundantly available and any loss of compressed air can be immediately replenished. Although air brake have an advantage over hydraulic brakes, their performance is sensitive to maintenance, and can degrade significantly under poor maintenance [3]. Improper maintenance leads to the leakage of compressed air and the out-of-adjustment of pushrod in the air brake system. In the following subsections, these two faults are discussed further.

1. Leak

Leak may be defined as a loss of air in the air brake system. The leakage of compressed air occurs due to any of the following reasons or their combinations: rupture of the hoses carrying compressed air, rupture of the brake chamber diaphragm, failure of the compressor, faulty / loose couplings etc. Experimental data shows that, there is a reduction in the steady-state brake chamber pressure due to the loss of compressed air. The reduction in the brake pressure leads to a reduced braking torque at the wheels of the vehicle. Apart from this, a leak causes an increase in the lag of the braking pressure response, thereby increasing the stopping distance of the vehicle. Figure 1 shows pressure transients in the brake chamber corresponding to different

leakage rates in the brake system and displays the lag in the pressure transients due to air leakage which increases the time taken to reach the effective brake chamber pressure (minimum braking pressure) during partial braking. An increase in the lag of the pressure response stems from the reduced mass flow of air into the brake chamber resulting from the leak. (For example, if there is a leak in a truck traveling at $\approx$ 27 m/s(60 mph), a lag of 0.1 sec in the pressure rise, leads to an increase in the desired stopping distance by 2.7 m (9 feet)).

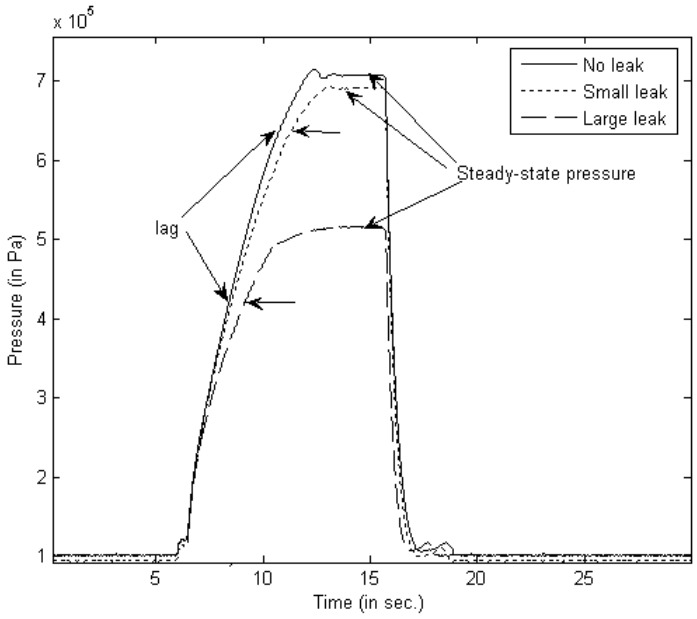

Fig. 1. Effects of leak on brake chamber pressure transients

2. The out-of-adjustment of pushrod

The friction between the brake pads and the brake drum causes the vehicle's kinetic energy to be dissipated as thermal energy, which causes the vehicle to stop. Consequently, the drum expands because of conduction of thermal energy through the brake drum. This increases the clearance between the brake pads and the brake drum

which, in turn, increases the steady-state stroke of the pushrod. In case of repeated braking (usually performed while going down a slope), the dissipation can be sufficiently large causing the clearance to increase to an extent that the pushrod stroke exceeds its safe limit[4]. This can lead to a sudden loss of braking torque at the wheels of the vehicle. Friction between the brake pad and the brake drum is another major cause of out-of-adjustment of the pushrod. Due to friction, the brake pads undergo mechanical wear which permanently changes the clearance between the brake pads and the brake drum. An increase in the clearance between the brake pad and the drum increases the stroke of the pushrod. The effect of the change in clearance on the braking force is shown in Figure 2. Also, a change in the pushrod stroke due to a change in the clearance leads to an increase in the steady-state stroke of the pushrod and in turn, increases the total volume of the brake chamber available for expansion. With more volume available for expansion of a given mass of compressed air, pressure rise in the brake chamber is slower. The effect of a change in the clearance is clearly visible in the brake chamber pressure transients and is shown in Figure 3. The response of braking, which includes the time delay and lag between the command and delivery of the brake torque at the wheels depends on the pressure transients with the response being slower for a large clearance/stroke. Clearly, the clearance dictates the braking response and in turn affects the stopping distance of the vehicles considerably.

---

[4]The braking force required to stop a commercial vehicle within a recommended safe distance (refer [4]) depends on several factors such as the speed of the vehicle, gross weight of the vehicle, road-tire interaction etc. This braking force depends on the stroke of the brake chamber pushrod and decreases rapidly for large values of the stroke of the pushrod (see Figure 2). The safe limit of the pushrod stroke is a value recommended in FMVSS 121 [4] and varies according to the type (effective area of brake chamber diaphragm) of brake chamber used in the air brake system.

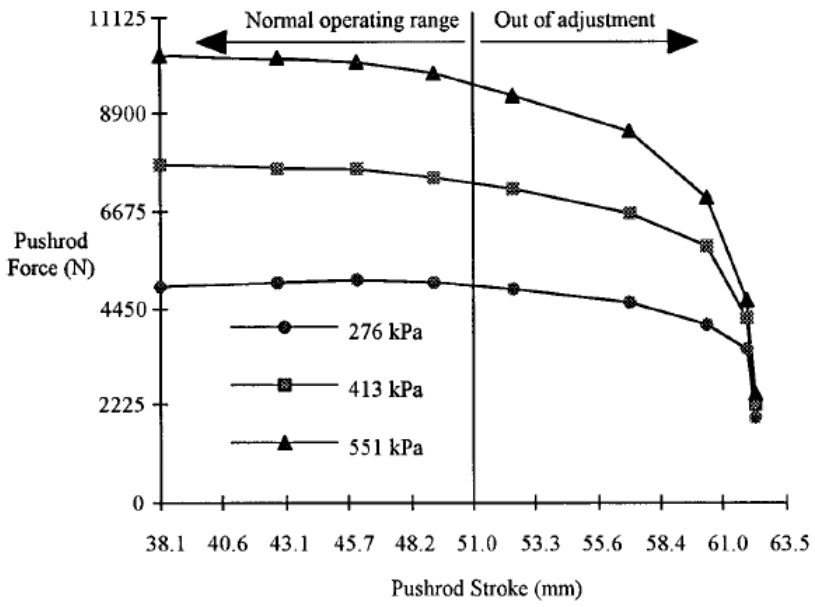

Fig. 2. Experimentally determined characteristics of pushrod force versus stroke [5]

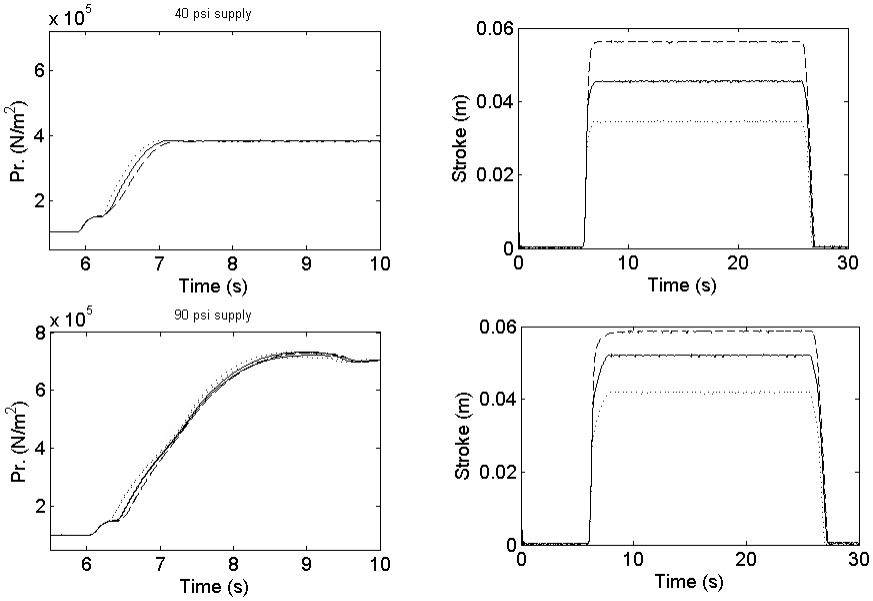

Fig. 3. Pushrod extension for different clearances and supply pressures

B. Motivation for the diagnostic schemes

The performance of air brakes in newly manufactured commercial vehicles in the United States is governed by Federal Motor Vehicle Safety Standard (FMVSS) 121 [4] and for "on-the-road" commercial vehicles by Federal Motor Carrier Safety Regulations (FMCSR) Part 393 [6]. Inspection techniques that are currently used to monitor the performance of air brake system are classified into two categories: "visual inspections" and "performance-based inspections" [3]. Visual inspections entail measuring the steady-state pushrod stroke and the thickness of the brake linings and detecting leaks in the brake system through aural and tactile means. They are subjective, time-consuming and difficult on vehicles with a low ground clearance. Performance-based inspections involve measurement of the braking force/torque, the stopping distance, the brake pad temperature, etc.

One may not be able to detect these faults unless brakes are inspected frequently. Preventive safety inspections such as the maintenance inspections conducted by fleet operators and enforcement inspectors involves them to typically go underneath a truck and check for the stroke of the pushrod and leaks in the brake system. They take up approximately 15-20 minutes of the 30 minutes spent on inspecting a brake during an enforcement inspection [3]. Federal Motor Vehicle Safety Standard (FMVSS) 121 [4] provides guidelines for the inspection procedure and it requires the full application of brake (corresponds to panic braking) at 90 psi supply pressure, during which the driver of the vehicle fully presses the brake pedal. Since the current inspection techniques are either unweilding, time-consuming or infrastructure intensive, there is a need for a diagnostic system that facilitates the inspection of air brakes. A large number of accidents, involving commercial vehicles, occur due to faults in the air brake system. Of the 37,261 casualties due to motor vehicle crashes in 2008, 4229 (11%) died in

crashes that involved a large truck [7]. Two prominent faults that have been reported are the out-of-adjustment of pushrod and the leakage of air in the brake system [8]-[13]. A study conducted by Federal Motors Carrier Safety Administration (FMCSA) showed that 26% of the total number of crashes reported in case of trucks occured due to faults in their air brake system [8]. Also, the average cost associated with an accident involving a commercial vehicle, as reported by FMCSA, is $59,153 [12].

Existing air brake systems on trucks have a warning device which alerts the driver of a presence of leak and is activated only when the reservoir pressure drops below 60 psi. The driver's role in the braking process is to meter the compressed air from the reservoirs to the brake chambers. The metering valve opening depends on the movement of the brake pedal by the driver. The driver has no tactile feedback about the braking performance of the vehicle unlike hydraulic brakes (used in passenger cars), where the driver gets feedback in the form of pressure on his/her foot. Upon the receipt of such a warning, the driver is expected to activate the emergency brakes, which results in the spring brakes being deployed at the rear wheels. The drop in the reservoir pressure below the threshold (known as the reservoir depletion) occurs due to ruptured air hoses, punctured reservoirs etc. and results in a significantly degraded braking performance. The rate at which compressed air leaks from the brake system, in this case, is so severe that the compressor is not able to replenish the loss of compressed air in the reservoir. But, in the presence of small leaks, the compressed air lost due to the leakage is usually replenished by the compressor and the pressure in the reservoir remains above the threshold. Hence, the warning device is never activated and the deteriorated performance of the brake system due to the leak remains undetected. Therefore, the driver remains oblivious of any change in the air brake system's performance due to the small leaks in the system, increasing the possibility of an accident to occur.

Lastly, none of the safety or performance-based tests can provide information concerning the speed of the brake response which is directly affected by the leaks and out-of-adjustment of the pushrod. From Figure 3, it is observed that even when the supply pressure is 40 psi, the pushrod strokes fully. Hence a measurement of pushrod stroke, during manual inspection, will not provide a complete picture of the health of the air brake system i.e. a presence of leak. However, the effect of change in the pushrod stroke in clearly visible in pressure transients in the brake chamber. Also, Figure 1 shows that the effects of leak are visible in pressure transients and on the steady-state pressure in the brake chamber. For these reasons, we measure pressure in the brake chamber as a signal for diagnosis of air brakes. In view of the limitations on the existing techniques for the leakage detection and for the out-of-adjustment of pushrod, there is a need for a diagnostic scheme to detect a leak which is not severe enough to activate the warning system, estimate its severity and estimate the pushrod stroke in an air brake system. A fast, reliable and accurate diagnostic scheme will reduce inspection times, manpower and costs involved in truck inspections.

C. Model based diagnostic system for air brakes

The basic structure of a model based diagnostic system is as follows:

1. A mathematical model of the system: The model enables one to predict the output of the system in response to specified inputs.

2. Measurement of output: The output of the system is measured using “reliable” sensors.

3. Computation of the residual: This task involves the comparison of the output predicted by the model and the output of the system measured by a sensor for

the same input. Clearly, if the two differ by a significant amount (threshold), one concludes that there is a fault. The determination of a threshold for a diagnostic system depends on the accuracy of a model representing the system, the reliability of sensors etc. Sometimes, residuals are processed further to diagnose faults.

Isermann [14] showed that the fault diagnosis of a DC motor can be performed by tracking the changes in the armature resistance of the motor. Benkherouf et al. [15]. found that the fault in the gas pipelines is reflected by change in the steady-state mass flow rate of gas, flowing through the pipelines. Similar approaches have been used, to detect faults in the system or a part of the system, by various researchers and for a variety of systems [16], [17]. A similar approach has been followed towards the development of fault diagnostic algorithms for the air brake system.

D. Air brake system - a "sequential" hybrid system

Hybrid nature is observed in many phenomena in nature as well as in systems that are a consequence of technological developments. The term "hybrid" signifies different things to different researchers. Researchers dealing with modeling the response of metals during melting and solidification, a phase change that not only can induce a change in symmetry of the material response but also can result in different governing differential equations depending on the constitutive assumptions about the response of the material. As an example, glass melting and solidification phases have been modeled as a hybrid system [18]. In case of air brake system, the "hybrid" nature stems from the system being in different modes of operation corresponding to different values of the displacement and is a result of different springs coming into contact with the pushrod in different ranges of displacement. Following are the modes of operation

- first mode when the pressure in the brake chamber is not sufficient to overcome the preload of the spring and initiate the motion of the piston. When pressure in the brake chamber is sufficient to overcome the preload of the spring, the pushrod begins to move and the air brake system transitions to the second mode. The system continues to be in the second mode as long as the brake pads are not in contact with the drum. The volume available for expansion of air is increasing in this mode. The third mode of operation starts once the brake pads have contacted the drum. It is in this mode that the air brake system delivers brake torque to the wheels. Due to compliance of the brake pads, the pushrod continues to move even after the pads contact the drum.

The air brake system is "sequential" in the sense that as the pressure rises, the displacement of the pushrod increases and the system transits through a distinct sequence of modes and upon a reduction in pressure, the sequence of modes is revisited in the reverse order. The modes of operation depending on the displacement of the pushrod are as shown in Figure 4.

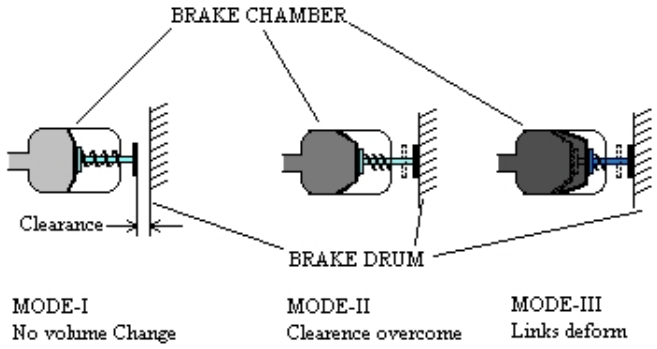

Fig. 4. Modes of operation of the air brake system [19]

E. Objectives of the dissertation

The main objective of this dissertation is to provide model based diagnostic scheme for estimating the severity of leak and out-of-adjustment of pushrod stroke. The diagnostic scheme for leak is based on a model developed for the mass flow rate of air leaking from the test setup at Texas A&M University. The mathematical model for the leak has been corroborated with the experimental data from the test setup.

The estimation scheme for the out-of-adjustment of pushrod is based on a model proposed for the stored energy in the brake chamber. Experimental data from the test setup for different strokes of the pushrod has been used to corroborate the estimation scheme for a single brake chamber.

Air brake system behaves as a typical hybrid system with its mode of operation depending on the clearance between the brake pad and the drum. For such systems, a scheme that estimates the states of a hybrid system without the knowledge of the parameters that govern the mode-to-mode transition(*clearance between the brake pad and the drum*) has been given.

F. Organization of this dissertation

The subsequent chapters provide a description of the air brake system test setup, the details of the work related to modeling and the development of the diagnostic schemes. A detailed description of the test setup and its instrumentation is given in Chapter II. A discussion on the development of the model for the mass flow rate of leak, the assumptions and corresponding model and the corroboration of the model, is given in Chapter III. In Chapter IV, a discusses is provided about the estimation scheme for pushrod and its corroboration with the data obtained from the test setup in various configurations. Estimation scheme for a class of hybrid systems, such as

the air brake system, is given in Chapter V. Finally, conclusions on various results that were obtained during the course of this dissertation and the scope of future work are given in Chapter VI.

CHAPTER II

AIR BRAKE SYSTEM

The earliest account on the application of air brakes has been in the railway industry. Prior to the introduction of air brakes, trains used a primitive brake system that required an operator in each car to apply a hand brake at the signal of the train director or engineer. This inefficient manual system was replaced by direct braking using the air brake system, which provided an efficient and reliable braking in the trains [20]. George Westinghouse in 1869 developed and patented the first practically applicable air brake system in railways [21]. It was not until 1919 that air brakes were introduced in trucks with a modified design by George Lane [22]. With the passage of time, there have been several modification in the design of various components and the air brake system as whole to the one in modern commercial vehicles.

A. Air brake system in modern commercial vehicle

The air brake system in modern commercial vehicles consists of a pneumatic subsystem and a mechanical subsystem. The pneumatic subsystem consists of a compressor, a storage reservoir, pneumatic valves, a brake chamber and the hoses connecting them. The pneumatic subsystem is divided into the primary circuit and the secondary circuit, as shown in Figure 5. This design layout, also called as dual-circuit layout, ensures fail-safe operation of the air brake system. In the event of failure of particularly one of the circuits, the other circuit can still perform a partial braking action. The mechanical subsystem consists of a brake chamber, a pushrod, a slack adjuster, an "S" shaped cam, brake pads and a brake drum as shown in Figure 6. As compressed air enters the brake chamber, it expands and pushes the diaphragm and pushrod, causing it to rotate the slack adjuster. The slack adjuster, in turn, rotates

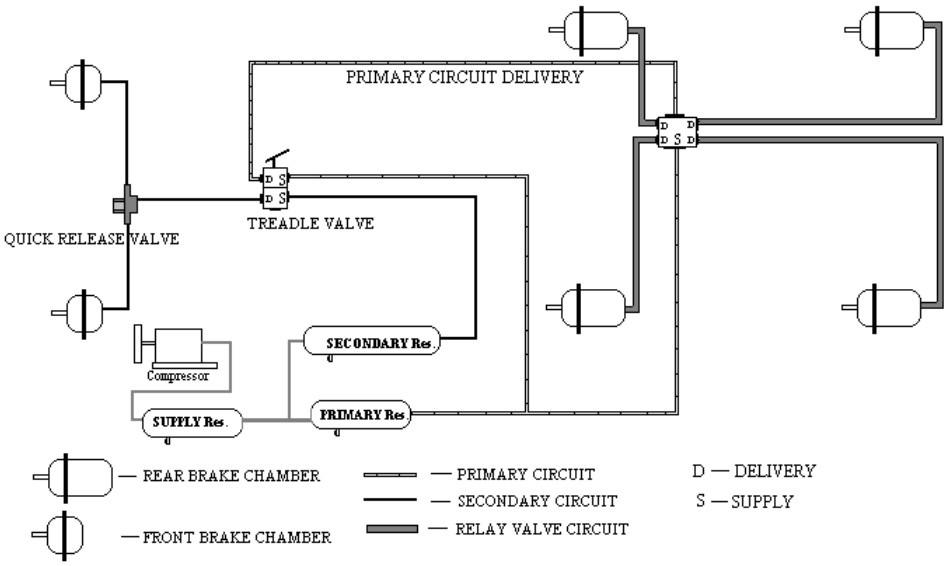

Fig. 5. A simplified layout of air brake system for a tractor

the S-cam as it is connected to the S-cam through a splined shaft. The rotational motion of the S-cam pushes the brake pads against the brake drum, causing the braking action.

The working of components of the pneumatic and the mechanical subsystems of the air brake system is discussed next.

1. **Brake chamber:** A brake chamber is a mechanical system consisting of a spring, a piston and pushrod (connected to the piston) and a diaphragm, arranged as shown in Figure 7 and converts energy from compressed air into the linear motion of the pushrod. The force transmitted along the pushrod is directly proportional to the pressure of compressed air in the brake chamber. The brake chambers are specified according to their effective cross-sectional area of their diaphragm; for example, a "type 20" brake chamber (used in front axle) has a cross-sectional area of 20 in^2 (0.0129 m^2). The rear axle brake chambers ("type 30") are specially modified to include a safety mechanism, also known

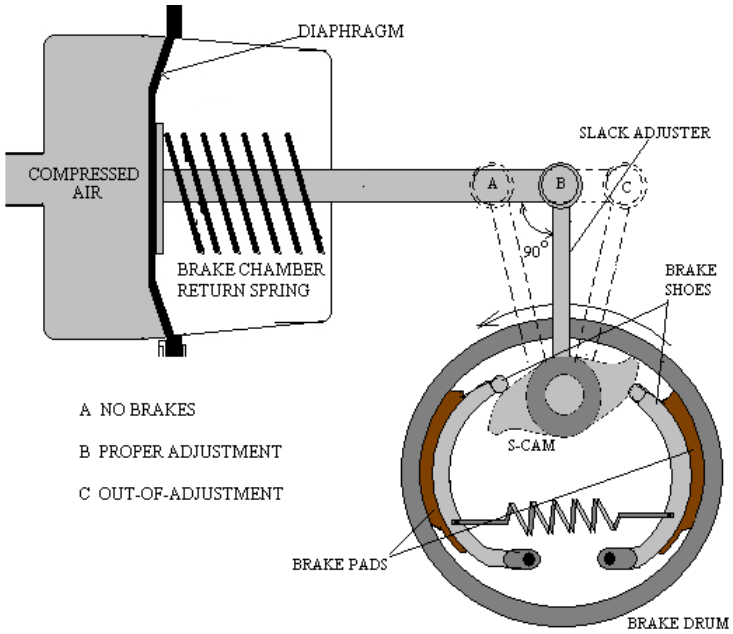

Fig. 6. S-cam foundation brake

as the emergency brakes. The emergency brakes are used by the driver, to assist in braking, only when the leak warning devices are activated in the vehicle [23], [24]. The emergency brakes are automatically deployed when the reservoir pressure drops below 40 psi (377.156 kPa abs.).

2. **Compressor and reservoirs:** A compressor is a mechanical device that uses mechanical energy to compress air from atmospheric pressure to the rated supply pressure and is the most important component of the air brake system. The compressor is driven directly by the engine of the vehicle and has a governor that controls the flow of compressed air to the reservoirs. In case the reservoirs are filled to their rated capacity (rated pressure), the governor cuts-off the flow of air to the reservoirs, from the compressor, until the reservoir pressure drops below the cut-off pressure (usually 100 psi). The moisture in the compressed air is filtered by allowing the compressed air to pass through a series of air driers,

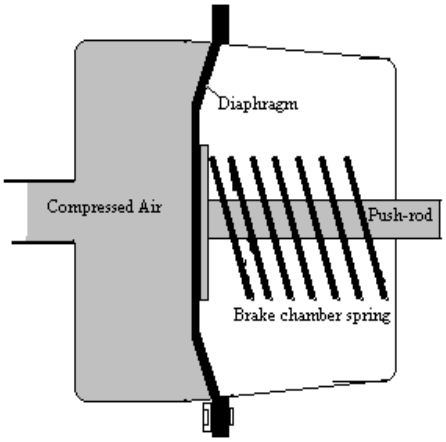

Fig. 7. Brake chamber

before being stored in the reservoirs. This is done to prevent any degradation of the components of the air brake system by the moisture.

The air brake system has two reservoirs, the primary reservoir and the secondary reservoir. The primary reservoir supplies compressed air to the primary circuit and the rear brake chambers. The secondary reservoir supplies air to the front brake chambers and for disabling the emergency / parking brakes, during normal working of the air brake system. According to FMVSS 121, the combined volume of all the reservoirs should be atleast 12 times the combined maximum volume of all the brake chambers of the air brake system.

3. **Treadle valve:** The treadle valve consists of the primary valve and the secondary valve, as shown in Figure 8. The primary valve opening depends on the displacement of the plunger in the treadle valve. The displacement of the plunger is proportional to the brake pedal displacement and the pressure in the primary circuit. Pressure in the primary circuit is responsible for the actuation of metering valve (the secondary valve) for the brake chambers on the front

axle of the vehicle and the metering valve for the brake chambers on the rear axles. In the event of a failure of the primary circuit, the secondary valve can be directly opened by the displacement of the plunger, which then initiates partial braking in the front axle.

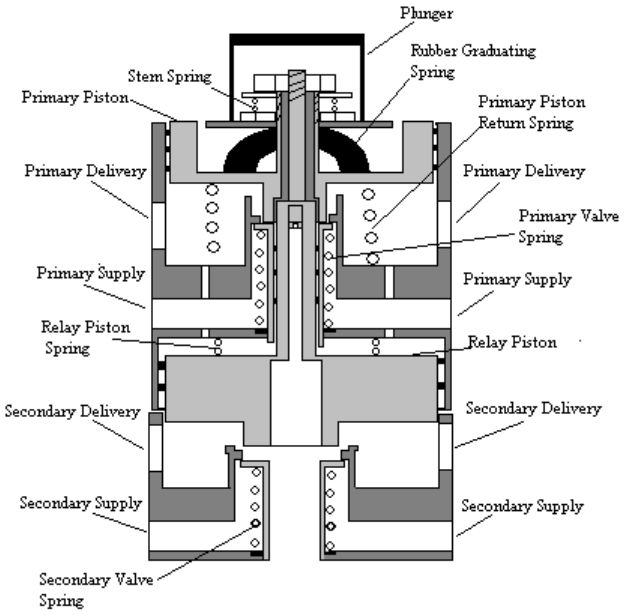

Fig. 8. Treadle valve

4. **Quick release valve and relay valve:** The quick release valve is mounted on the front axle and air flows to the front brake chambers through it. The main function of the quick release valve is to ensure quick exhaust of air from the front brake chambers as soon as the brake pedal is released by the driver. The relay valve is mounted on the rear axles and acts as the metering valve to the rear brake chambers. The opening of the relay valve is controlled by the pressurized air in the primary circuit which pushes the diaphragm (see Figure 9) that in turn opens the relay valve. The supply to the relay valve is directly from the primary reservoir. One of the primary reasons to have a relay valve in the air

brake system is to reduce the delay between the actuation of rear brakes and the actuation of front axle brakes during braking.

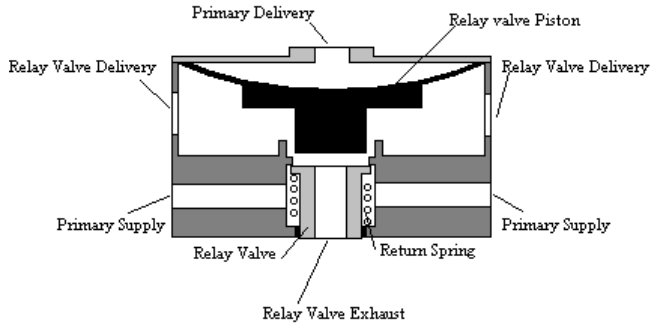

Fig. 9. Relay valve assembly

5. **Slack adjuster:** The main function of a slack adjuster is to convert the linear motion of the pushrod into the rotational motion of the S-cam, as shown in Figure 6. Ideally, the maximum force (in steady-state) is transmitted through the pushrod to the S-cam when the angle between the pushrod and the slack adjuster is 90^o. This force is then transmitted to the brake pads and results in contact between the brake pad and the brake drum. However, due to a misalignment during assembly or the mechanical wear of the brake pads the angle tends to deviate from the optimal valve (90^o) which causes a reduction in the force transmitted in steady-state. In order to rectify the misalignment, a realignment mechanism is provided in the slack adjuster. This mechanism can be operated using the adjusting nut as shown in Figure 10. In modern slack adjusters, the realignment takes place automatically but only for a certain degree of misalignment.

6. **The brake drum assembly:** The brake drum assembly consists of a splined shaft that is connected to the slack adjuster, an "S" shaped cam mounted

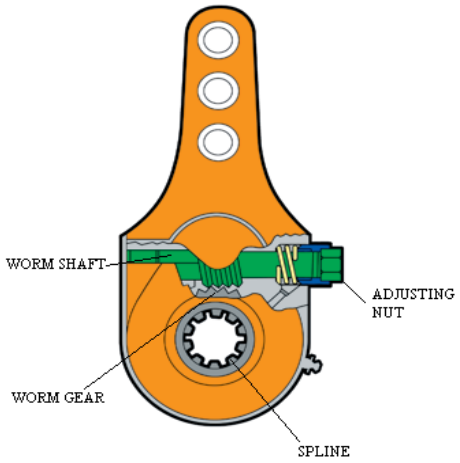

Fig. 10. Layout of a slack adjuster

connected to the splined-shaft, the brake pads which are actuated by the "S"-cam, the brake drum, as shown in Figure 11. The slack adjuster transmits the pushrod force to the brake pads through the S-cam, which in turn pushes the brake pads against the brake drum and causes the braking action. Brake pads are hinged about a pivot and are held in a retracted position (no contact with the drum) by a return spring, when braking is not needed. They are made up of high friction material that has a low coefficient of thermal expansion. The brake drum is made up of cast iron and has the friction material covering the area against which the brake pads make contact. This kind of arrangement of the brake pads and the brake drum has a self-energizing (or more appropriately "self-applying") characteristics i.e., depending on the direction of rotation, one of the brake pads is further forced into the drum surface by the moment due to friction but leads to uneven wear of the brake pads. One of the major disadvantages of this construction is the phenomenon of brake fade which occurs when brakes are applied frequently, causing a sudden loss of braking force. The loss of braking force is due to the loss of frictional force between the brake pads

and the brake drum, at high temperatures due to the inefficient transfer of heat that is generated during braking.

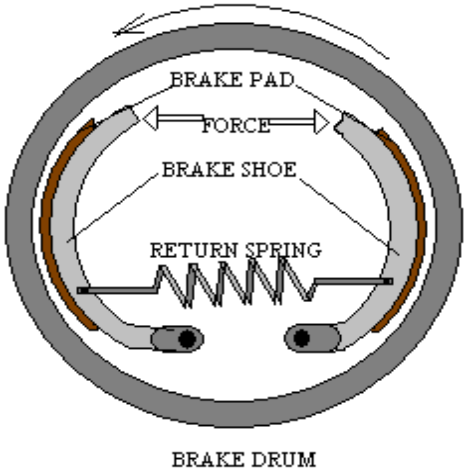

Fig. 11. A layout of a brake drum

B. The experimental setup

An experimental setup that closely resembles the actual air brake system in a commercial vehicle was built at Texas A&M University and is shown in Figure 12. The setup has two "type 20" front brake chambers on the front axle and two "type 30" spring brake chambers mounted on a fixture that simulates the rear axle, as shown in Figure 13. Air is supplied by a 5HP (3.73 kW) air compressor - stored in the primary reservoir and by a 2 HP (1.49 kW) compressor - stored in the secondary reservoir, as shown in Figure 13. Pressure regulators are installed at the delivery side of the reservoir to control the air pressure supplied to the system and to ensure constant upstream (supply) pressures during the tests. A dual brake valve (treadle valve) serves as the input to the braking system.

The treadle valve is actuated using an electromechanical actuator with position feedback [25]. The actuator is controlled by a servo drive/controller. Pressure trans-

Fig. 12. Experimental setup at Texas A&M University

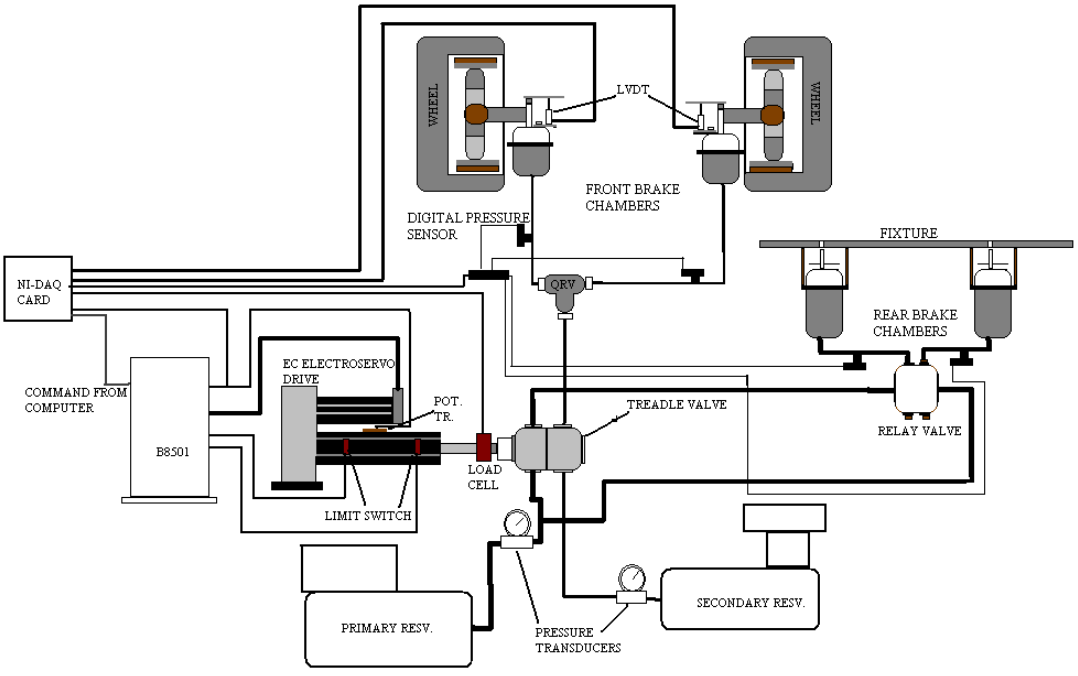

Fig. 13. A schematic of the experimental facility

ducers are mounted at the entrance of all brake chambers to record the pressure transients. Also, a displacement transducer was mounted on each brake chamber to measure its pushrod stroke during test runs. All the sensors were interfaced using a Data Acquisition (DAQ) card mounted on a PC for data collection during the test runs. The desired treadle valve plunger motion is the input from the computer to the servo drive (B8501 [26]) through the DAQ card. A MATLAB/Simulink application records and analyzes the data.

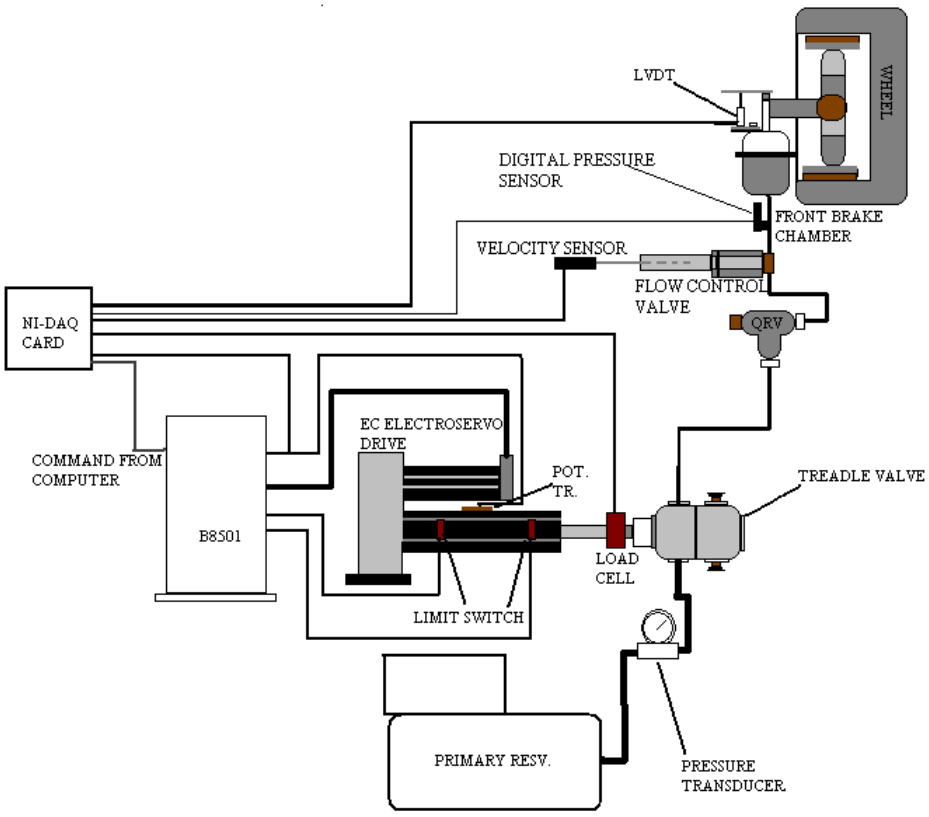

Fig. 14. A schematic of the experimental facility for leak test

A schematic of the setup to perform leak experiments is shown in Figure 14. The primary delivery of the treadle valve was directly connected to the front brake chambers for all test runs for leak. Leak has been simulated using a flow control

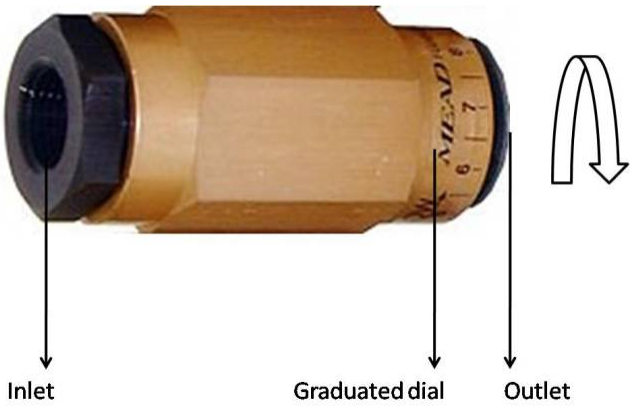

Fig. 15. Flow Control Valve

valve (FCV) [27]. The flow control valve used in the experimental setup is shown in Figure 15. The valve opens fully upon four complete turns of the graduated dial. The valve is installed between the primary delivery and the brake chamber as shown in Figure 14. Severities of leak are simulated by turning the dial of the FCV by half-a-turn (1/8 FCV), one full turn (1/4 FCV), two full turns(1/2 FCV) etc. In order to measure the mass flow rate of leaking air, a velocity sensor has been used. The sensor is interfaced with the computer for data acquisition using the DAQ card. The sensor gives a voltage output equivalent to the measured velocity, which is recorded during the test runs. The outputs from the velocity sensor are then converted to dynamic pressure using the calibration curve of the sensor. This pressure data can be converted to mass flow rate using suitable scaling factors. The components of the test setup, the sensors used in the setup and their respective specifications are listed in Table I.

Table I. Details of the components used in the test setup at Texas A&M University

Component	**Manufacturer**	**Model no.**	**Details**
Primary compressor/reservoir	Campbell Hausfeld	WL651300AJ	Capacity: 12 gal. (0.0454249 m^3)
Secondary compressor/reservoir	Campbell hausfeld	FP200200AV	Capacity: 6 gal. (0.02271 m^3)
Pressure Regulator	Omega Engg.	PRG50120	Pressure range: 2-120 psi (115.1-928.8 kPa)
Treadle Valve	Bendix	E-7	Regulates brake chamber pressure
Quick release Valve	Bendix	QR-1	Allows quick pressure release in front brake chambers
Relay Valve	Bendix	R-12	Meters compressed air rear brakes chambers
Brake Chambers	Bendix	Type-20 and Type-30	Converts pressure to force
Flow Control Valve	Mead Fluid Dynamics		Simulates leak opening in the test setup
Velocity Transducer	All Sensors	7E23-2	Measures velocity of leaking air
Linear pot.	Omega Engg.	LP802-75 LP802-100	Max. stroke: 76.2 mm Max. stroke: 101.6 mm
Pressure Transducer	Omega Engg.	PX181-100G5V	Max. range: 689.5 kPa gauge
Data Acq. Board	National Instruments	PCI-MIO-16E-4	Has 8 differential analog input and 2 analog output channels
Electro-mechanical actuator	IDC	EC2-B23-20-05B-50-MSI/ MS6E-MT1E-L	Actuates the treadle valve plunger with a max. stroke of 100 mm.
Servo drive controller	IDC	B8501	Actuator controller

CHAPTER III

DETECTION OF AIR LEAKAGE AND MODEL BASED ESTIMATION OF ITS SEVERITY

In this chapter, a model based diagnostics of leak in the air brake system will be discussed. A model for the mass flow rate of the leakage of air has been developed and corroborated with the experimental data obtained by simulating varying severities of leak in the test setup. A diagnostic scheme for leak, based on this model, has been implemented in form of a look-up table.

A. Existing models for a *"leak-free"* air brake system

Most of the models that have been developed for the air brake system assume the system to be without any faults (no leaks) [28]-[33]. The governing equations for an air brake system are mode dependent, i.e., the governing equations change with the modes of operation of the air brake system. These models predict pressure transients in the brake chamber and the steady-state stroke of the pushrod. The model by Acarman et al. [31] predicts pressure in the brake chamber during the pressure-rise mode, the pressure-hold mode and the pressure-decay mode of the air brake system. Kandt et al. [32] fit an exponential for pressure measurements during the exhaust phase (pressure-decay mode).

However, most of these models ignore the driver's input, which controls opening of the treadle valve. A mode dependent model, that includes the input from driver, has been developed by Subramanian et al. [33]. Three modes of operation are assumed - the first mode is when the pressure in the brake chamber has not risen enough to overcome the preload of the spring and initiate the motion of the pushrod. In the second mode, pressure in the brake chamber is sufficient to overcome the preload of

the spring and initiate the motion of pushrod; however, the brake pads are not in contact with the drum. In this mode of operation, the volume available for expansion of air is increasing. Once the brake pads have contacted the drum, the air brake is in the third mode and it is in this mode that the air brake system delivers brake torque to the wheels. Because of compliance of the brake pads, the pushrod can continue to move while the pads contact the drum. Figure 16 shows the state of the air brake system in each of these modes and the measured pressure transients in the brake chamber during these modes are shown in Figure 17. Since the operation of air brakes is mode dependent, the mathematical model desired is a hybrid system (discussed in Chapter VI).

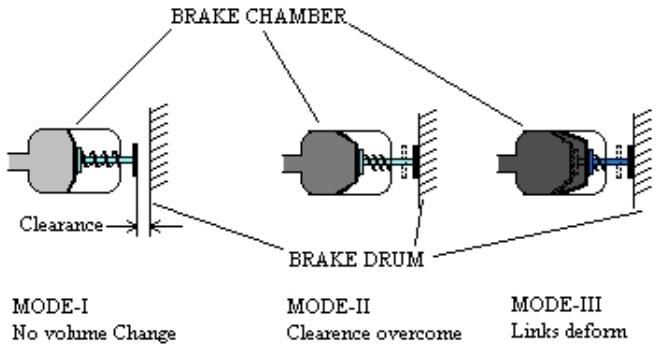

Fig. 16. Modes of operation of the air brake system [19]

The mode dependent model for the air brake system that includes the driver's input is discussed in the following section.

1. A mode dependent model for air brake system with the driver's input

The governing equations of the model have been developed using the following assumptions:

1. Friction at all sliding surfaces of the valves may be assumed to be negligible

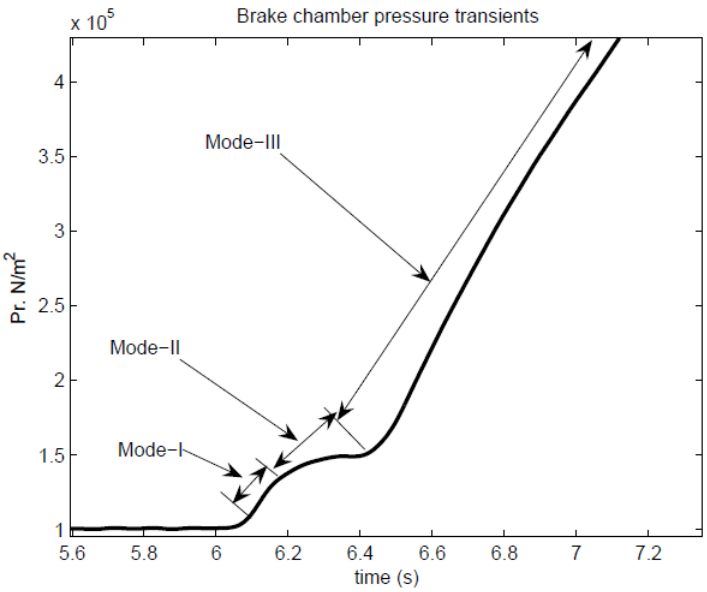

Fig. 17. Pressure transients in a brake chamber during various modes of operation

since all components were well lubricated.

2. Inertial forces were assumed to be small compared to the pressure forces and spring forces.

3. The opening of the treadle valve may be assumed to behave like a nozzle.

4. Thermal properties in the supply chamber of the treadle valve were assumed to be the stagnation properties for the inlet of the nozzle.

5. Flow through the treadle valve opening was assumed to be one-dimensional and isentropic [34], [35].

6. Air was assumed to behave like an ideal gas with constant specific heats.

7. Uniform fluid properties were assumed at all sections in the nozzle.

8. Friction losses in the hoses were neglected.

9. Compressibility effects of air in the hoses were ignored as the Mach number was found not to exceed 0.2 [33].

The constitutive equation of ideal gas law relates the brake chamber pressure, the brake chamber volume and the mass of air in the brake chamber, at any given time instant. The brake system has been assumed to be without any leaks. Therefore, the mass of air coming out of the treadle valve is same as the mass of air flowing into the brake chamber.

Applying the principles of conservation of mass and energy in the pneumatic subsystem, the governing equations for pressure transients in the brake chamber for each of its modes have been determined and are as follows:

$$C_D \frac{P_b}{RT_b} A_p U_E = \begin{cases} \left(\frac{V_{o1} P_0^{\frac{\gamma-1}{\gamma}}}{\gamma R T_0 P_b^{\frac{\gamma-1}{\gamma}}} \right) \dot{P}_b, & \text{if } P_b < P_{th}, \\ \left(\frac{V_b P_0^{\frac{\gamma-1}{\gamma}}}{\gamma R T_0 P_b^{\frac{\gamma-1}{\gamma}}} + \frac{P_b^{\frac{1}{\gamma}} A_b M_1 P_0^{\frac{\gamma-1}{\gamma}}}{R T_0} \right) \dot{P}_b, & \text{if } P_{th} \leq P_b < P_{ct}, \\ \left(\frac{V_b P_0^{\frac{\gamma-1}{\gamma}}}{\gamma R T_0 P_b^{\frac{\gamma-1}{\gamma}}} + \frac{P_b^{\frac{1}{\gamma}} A_b M_2 P_0^{\frac{\gamma-1}{\gamma}}}{R T_0} \right) \dot{P}_b, & \text{if } P_b \geq P_{ct}. \end{cases} \tag{3.1}$$

The details about the parameters of (3.1) are given in Table II. The input to this model is the mass flow rate of air coming out of the treadle valve. This mass flow rate depends on the area of opening of the treadle valve. A lumped parameter approach[1] has been used to obtain the model that predicts the area of opening of the treadle valve. Friction in the mechanical components of the treadle valve has been neglected. The model uses the driver's input in the form of treadle valve plunger displacement to predict the area of the treadle valve opening. The predicted area can then be used to compute the mass flow rate of air coming from the reservoir and is the input

[1]It is expected that the final predictions of the model will not match the measurements due to this assumption. However, the steady state predictions are expected to match reasonably well.

Table II. Nomenclature of parameters used in the governing equations [33], [36]

Parameter	Description	Value (units)
γ	Ratio of specific heats for air	1.4
R	Gas constant for air	287 J/kgK
T_0	Stagnation temperature	293 K
P_b	Local pressure inside the brake chamber	Pa
T_b	Local temperature inside the brake chamber	K
U_E	Velocity of air coming out of treadle valve	m/s
P_0	Supply pressure	722 kPa
A_p	Area of treadle valve opening	m^2
C_D	Coefficient of discharge	0.82
V_{01}	Initial volume of air in brake chamber	$0.00032274m^3$
P_{th}	Push-out pressure	$\approx 120kPa$
V_b	Volume of air inside the brake chamber	m^3
A_b	Area of brake chamber diaphragm	0.0129 m^2
M_1	Calibration constant	$1.419 \times 10^{-6} m/Pa$
M_2	Calibration constant	$2.341 \times 10^{-8} m/Pa$
P_{ct}	Brake pad contact pressure	$\approx 151.2kPa$

to the model for pressure transients. The details regarding the model that predicts the area of the treadle valve opening can be seen in the paper by Subramanian et al. [33]. Collectively, the model for pressure transients and the treadle valve model will be referred to as the "leak-free" model in the rest of the dissertation. This is the starting point in development of a model for the air brake system in the presence of leaks. In Figure 18, one can see the pressure transients predicted by (3.1) when compared with the measured brake chamber pressure.

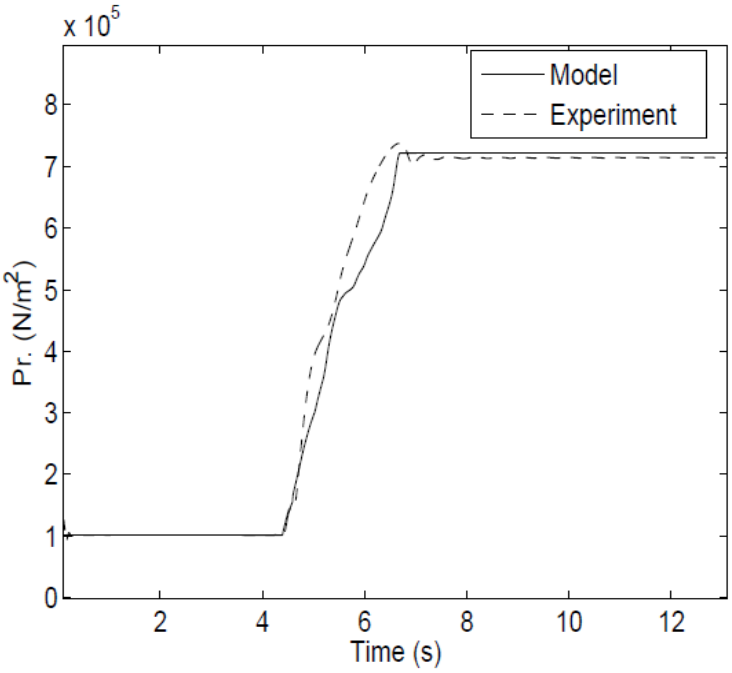

Fig. 18. A comparative plot showing the pressure predicted by the leak-free model and the measured pressure

In the presence of a leak, reduced mass flow rate of air flows into the brake chamber and the reduction in the flow rate is same as the mass flow rate of leaking air. The mass flow rate input to the model for pressure transients, in the presence of leak, is obtained by subtracting the mass flow rate of leaking air from the mass flow rate of air coming out of the treadle valve. A model for the mass flow rate of leaking

air has been developed [37] and a discussion regarding this model is given next.

B. A model for the mass flow rate of leaking air

For the purposes of developing a model, the leak is assumed to be near the brake chamber and past the treadle valve. The opening through which air leaks is assumed to behave like a nozzle. Air leaks to the atmosphere and the ratio of the supply pressure to the atmospheric pressure is greater than the critical pressure ratio[2]. Therefore, choked flow conditions have been assumed. Experiments showed that the mass flow rate of leaking air increased with the supply pressure and also with the area of leak (determined by the number of turns of the FCV), as shown in Figure 19. Similar assumptions have been made while developing a model for the mass flow rate of air leaking out of the engine manifolds by Nyberg et al. [38]. A functional form for the mass flow rate of leaking air in the air brakes has been assumed:

$$\dot{m}_{leak} = C_d A_l \frac{P_{sup}}{\sqrt{RT}} \sqrt{\gamma \left(\frac{2}{\gamma+1}\right)^{\left(\frac{\gamma+1}{\gamma-1}\right)}}, \tag{3.2}$$

where C_d is coefficient of discharge of a nozzle, A_l is the area of leak and P_{sup} is pressure in the brake chamber, R is gas constant for air, γ is the ratio of specific heats of air and T is temperature of the surrounding air. A parameter that relates the mass flow rate of leaking air to the steady-state brake chamber pressure has been obtained. This parameter may prove to be useful in the case of an actual vehicle, where the area of leak may not be known.

[2]Choked flow occurs when the ratio of the absolute upstream pressure to the absolute downstream pressure is equal to or greater than $\left(\frac{\gamma+1}{2}\right)^{\frac{\gamma}{\gamma-1}}$. This ratio is known as critical pressure ratio. γ is the ratio of specific heats of the gas [35].

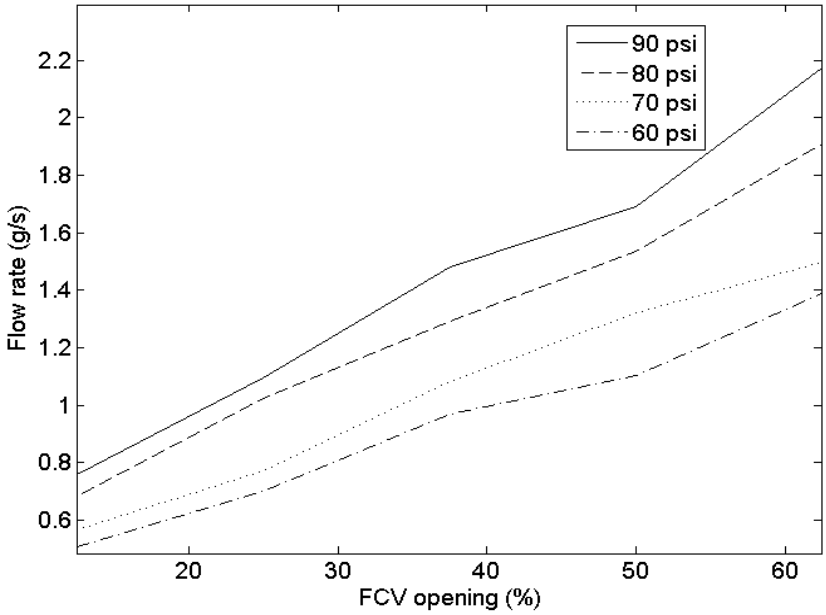

Fig. 19. Measured mass flow rate of leaking air for various supply pressures

1. Parameter of the mass flow rate model and its estimation

The mass flow rate of leaking air is related to the brake chamber pressure by (3.2). The parameter K that relates leak severity to the break chamber pressure has been defined as follows:

$$K = \frac{C_d A_l}{\sqrt{R}} \sqrt{\gamma \left(\frac{2}{\gamma + 1} \right)^{\left(\frac{\gamma+1}{\gamma-1} \right)}}. \tag{3.3}$$

Hence (3.2) ,ay be expressed as:

$$\dot{m}_{leak} = \frac{K P_{sup}}{\sqrt{T}}. \tag{3.4}$$

Therefore, if parameter K were known, the severity of leak can be computed from (3.2). The parameter has been obtained by minimizing least-square error ϵ which is given as follows:

$$\epsilon = \sum_{i=1}^{N} \left(\dot{m}_{meas}(i) - K \frac{P_{sup}(i)}{\sqrt{T}} \right)^2, \tag{3.5}$$

where N is the total number of measurement samples, i is the sample number, $\dot{m}_{meas}$ is the measured mass flow rate of air leaking from the flow control valve. The parameter K was found for leak measurements performed at different supply pressures (90 psi, 80 psi etc) and at different FCV settings (half-a-turn, single turn, two turns etc) .

The least-square estimation algorithm [39] requires the values of $\dot{m}_{meas}$, P_{sup} and T, of which P_{sup} and T were measured using the pressure and temperature sensors in the test setup. The flow of leaking air in the air brake system is turbulent and to compute the mass flow rate, the following approach was adopted: A cylindrical pipe was connected to the output port of the FCV so that the leaking air flows through the pipe. The centerline velocity of the flow through the pipe was measured (Appendix A) and using the "one-seventh" power law approximation of velocity profiles, use the correction factor for the measured velocity was obtained [40]-[43]. Using the correction factor, the ratio of average velocity, $\overline{V}$ to the measured centerline velocity, U, is:

$$\frac{\overline{V}}{U} = \frac{49}{60}. \tag{3.6}$$

The mass flow rate of leaking air was computed using the following relation:

$$\dot{m}_{meas} = \rho_{air} A_{pipe} \overline{V}, \tag{3.7}$$

where $\dot{m}_{meas}$ is the computed value of mass flow rate of leaking air, ρ_{air} is the density of air at ambient temperature and A_{pipe} is the cross-sectional area of the pipe of diameter 10 mm used in the experiment. The estimated values of K for varying severity of leak and for different supply pressures are given in Table III. A complete set of estimates of K, for FCV turns ranging from $\frac{1}{2}(12.5\%)$ to $2\frac{1}{2}(62.5\%)$ and for supply pressure from 60 psi to 90 psi, has been given in Srivatsan et al. [37].

The model for the mass flow rate of leaking air has been used to obtain the model that predicts pressure transients in the brake chamber, in presence of a leak in the

Table III. Leak mass flow rates for a full brake application at different supply pressures

Supply Pressure (psi)	FCV Turns	$\dot{m}_{leak}$ (g/s)	K	Steady State Pressure(psi)
90	2	1.82	5.78×10^{-7}	85.78
90	2.5	2.35	7.65×10^{-7}	84.07
80	2	1.66	5.65×10^{-7}	76.77
80	2.5	2.06	7.58×10^{-7}	76.28
70	2	1.42	5.84×10^{-7}	67.14
70	2.5	1.62	7.77×10^{-7}	66.87

air brake system. A discussion about this model follows next.

C. "Leak" model and its corroboration

In absence of any leak in the air brake system, the mass of air coming into the brake chamber is same as the mass flow rate of air coming out of the treadle valve opening. Therefore, we have the following relation:

$$\dot{m}_{in} = \dot{m}_{BC}, \tag{3.8}$$

where (3.8) is same as (3.1). Using the model for the mass flow rate of leaking air (3.4), the mass flow rate of air flowing into the brake chamber in presence of the leak has been obtained. This mass flow rate of air acts as the input to the governing equations for pressure transients in the brake chamber, obtained for the "leak-free" model. The modified equation for pressure transients is given as follows [37]:

$$\dot{m}_{in} - K\frac{P_b}{\sqrt{T}} = \dot{m}_{BC}, \tag{3.9}$$

where K in (3.9) is known (from Table III) for the given opening of the flow control valve, $\dot{m}_{BC}$ is same as the right-hand side of (3.1). Equation (3.9) will be referred to as the "leak" model in the dissertation. Figure 20 shows pressure transients in the brake chamber as predicted by the "leak-free" model and the "leak" model respectively.

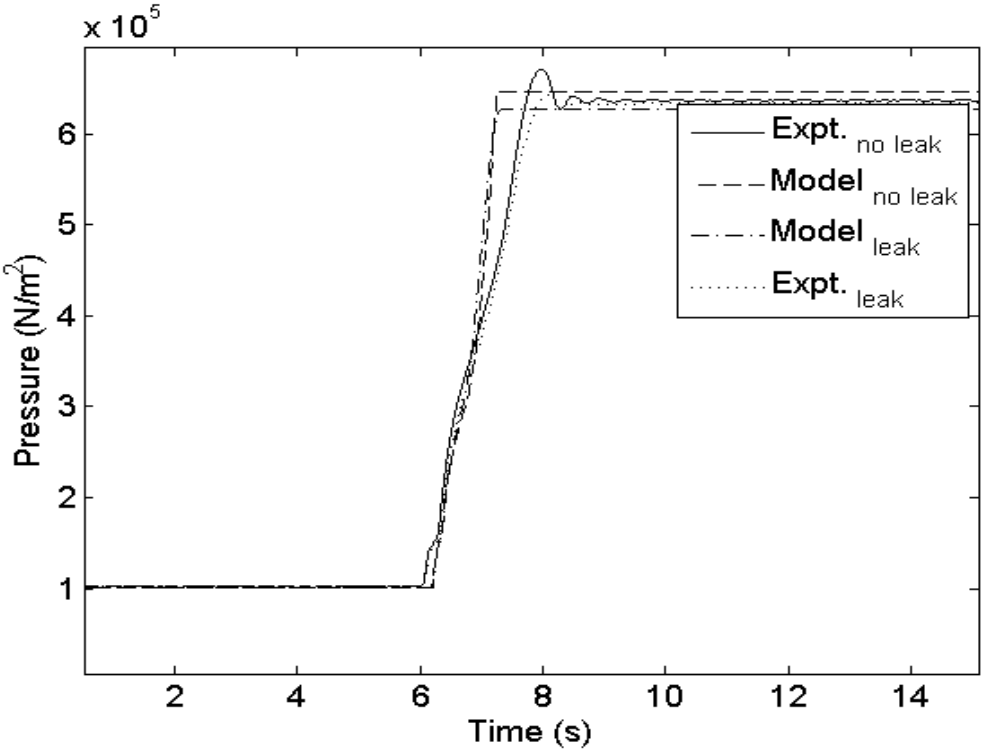

Fig. 20. A comparative plot of "leak-free" model and the "leak" model

The pressure transients predicted by numerically integrating (3.9) for varying severity of leak in the test setup, for different supply pressures, have been compared with experimental measurements in Figures 21, 22 and 23.

D. A look-up table based diagnostic scheme for leak

A diagnostic scheme has been developed based on Table III, by comparing the steady state pressure in the brake chamber to the supply pressure. The mass flow rate of

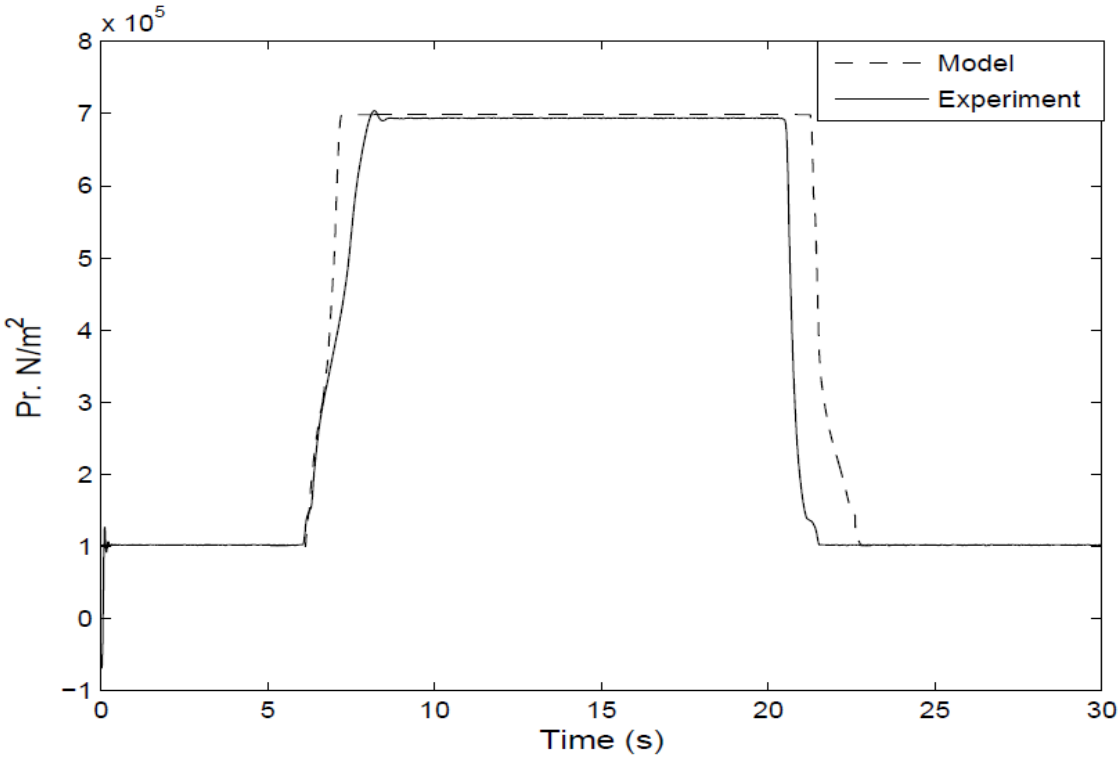

Fig. 21. Estimated steady-state brake chamber pressure for 90 psi (722 kPa) supply and for 2 turns of FCV

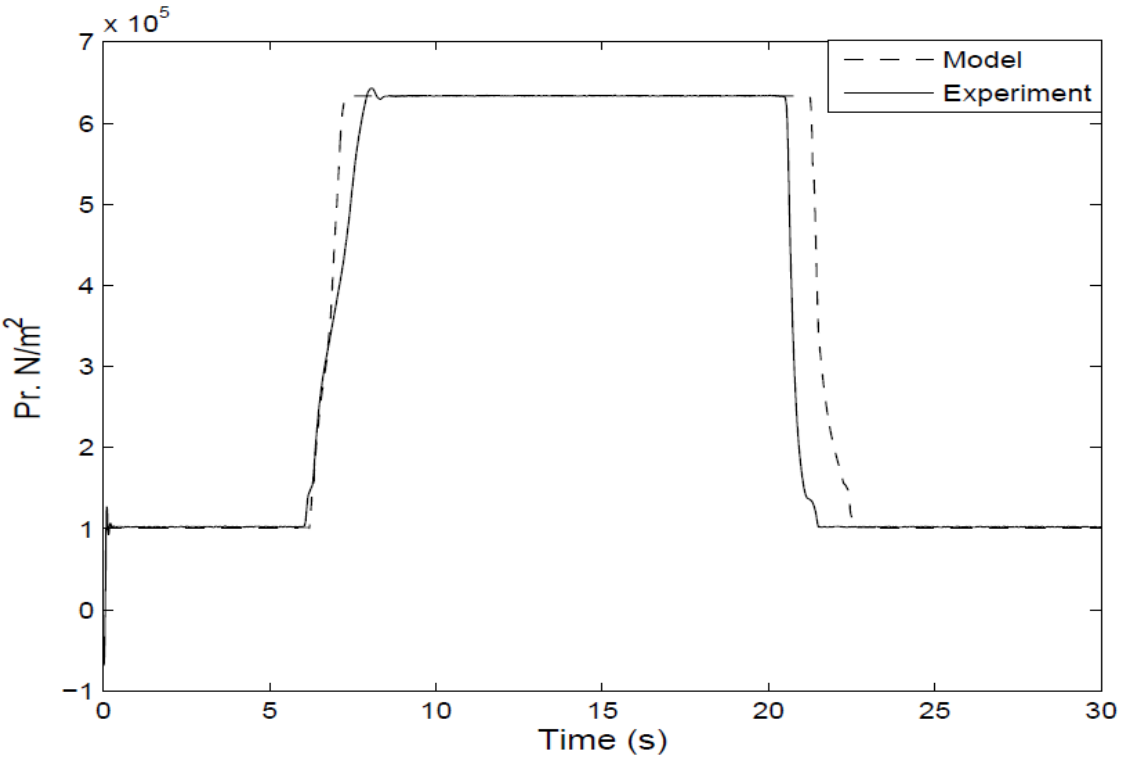

Fig. 22. Estimated steady-state brake chamber pressure for 80 (653 kPa) psi supply and for 2 turns of FCV

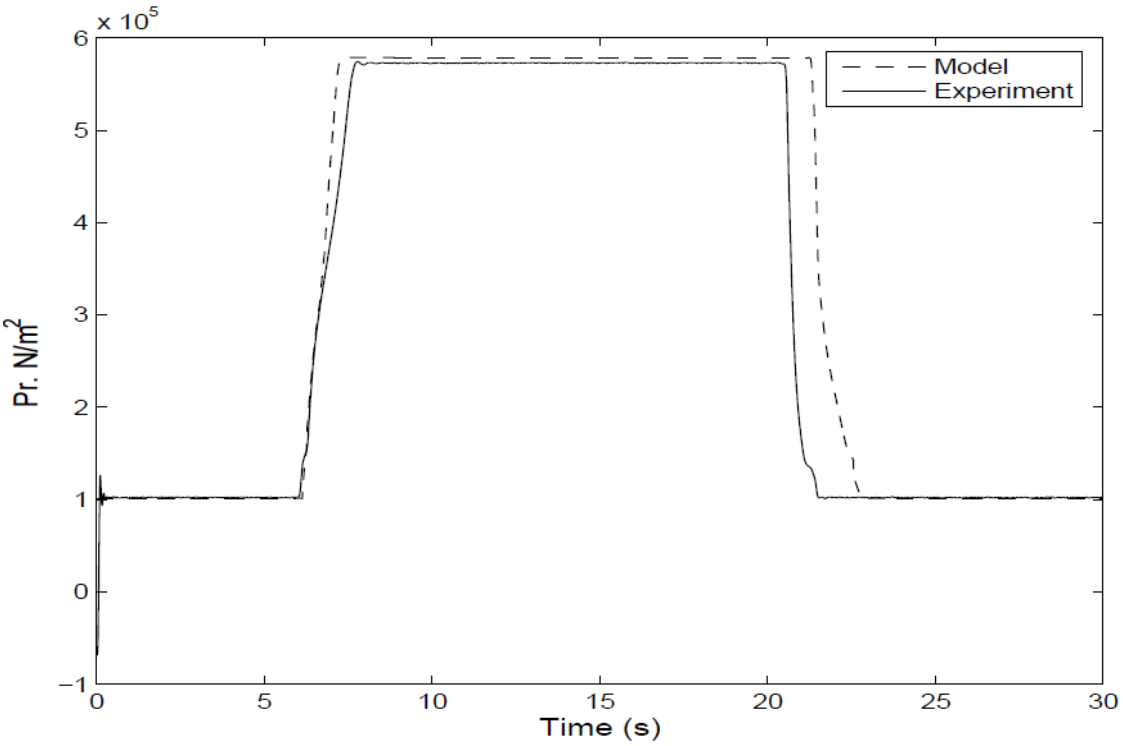

Fig. 23. Estimated steady-state brake chamber pressure for 70 psi (584 kPa) supply and for 1/4 turns of FCV

leaking air may be obtained from Table III depending upon reduction in the steady-state brake chamber pressure when compared with the supply pressure. One may alternatively determine the parameter K for leaks in an actual vehicle using Table III as a reference such that the steady-state pressure predictions from (3.9) match the measured brake chamber pressure. Different look-up tables may be required depending on vehicle configurations and component designs. Current results are for a typical straight truck or a 4×2 tractor configuration with data from the test setup at Texas A&M University with Bendix "E-7" treadle valve. Several full-scale tests need to be performed to verify whether a single look-up table will suffice or not.

CHAPTER IV

ESTIMATION OF THE STEADY-STATE STROKE OF PUSHROD

In this chapter, a discussion is provided about the scheme that has been developed for the estimation of steady-state stroke of the pushrod. The estimation scheme is based on a model that predicts the stored energy of the brake chamber. The scheme requires the measured brake pressure and the predicted steady-state brake chamber energy to estimate the steady-state stroke of the pushrod.

A. Existing schemes for estimation of the steady-state stroke of pushrod

Most of the existing schemes that estimate steady-state stroke of the pushrod of the air brake system are based on pressure measurements in the brake chamber. Kandt et al. [32] developed a scheme that is based on the pressure measurements during the exhaust phase (pressure-decay phase) of the brake chamber. The exhaust phase measurements have been considered in the scheme as this phase is independent of variations in the driver's input. The scheme is based on an exponential fit for the exhaust phase pressure measurements and a polynomial fit has been obtained that relates the steady-state pushrod stroke to the steady-state brake chamber pressure measurements and the time constant for the exhaust phase. Fuglewicz [44] developed a technique that gives real-time measurement of the pushrod stroke. However, the technique involves modifying the brake chamber so as to install a "hall-effect" displacement transducers directly on the brake chamber piston and the pushrod. The modification of the brake chamber may not be commercially viable for the air brake system manufacturers. Subramanian et al. [45] developed an estimation scheme based on the "leak-free" model of the air brake system. The scheme uses the "leak-free" model and measurement of pressure transients in the brake chamber to estimate the

contact pressure[1]. Experimentally observed variation between pushrod stroke and brake chamber pressure is shown in Figure 24. The contact pressure is the pressure at the point of inflection in the curve. A piece-wise polynomial fit relating the brake chamber pressure, the contact pressure and the pushrod stroke was determined from the experimental curve [36]. The steady-state pushrod stroke is computed by substituting the estimated contact pressure and the measured steady-state brake chamber pressure in the polynomial fit.

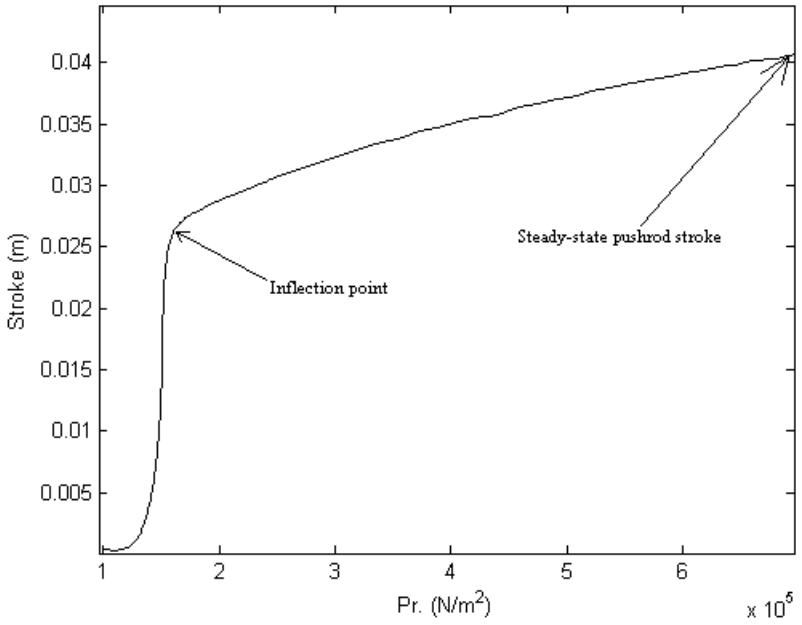

Fig. 24. Pushrod stroke vs. brake chamber pressure for a given clearance

However, experimental data shows that the steady-state pushrod stroke is highly sensitive to the change in contact pressure as shown in Figure 25. Therefore, a small error in estimating the contact pressure will lead to large errors in estimation of the

[1]The pressure at which the brake pads make contact with the drum.

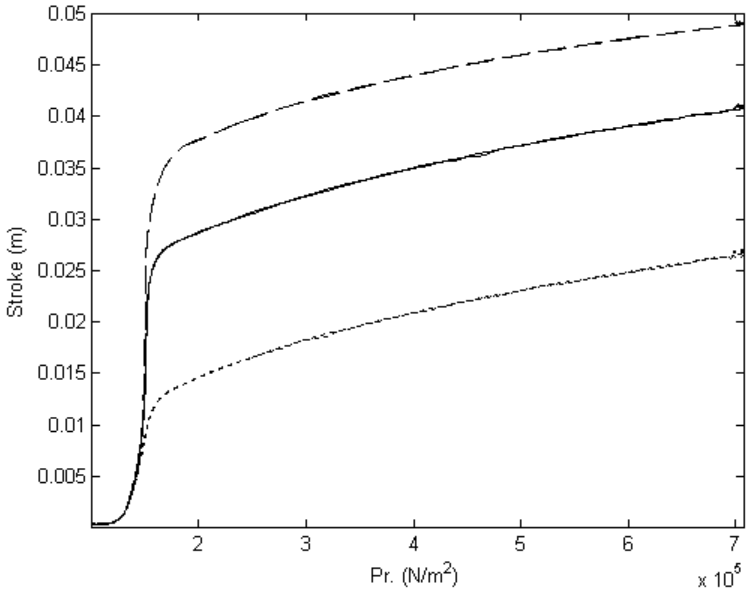

Fig. 25. Pushrod stroke vs. brake chamber pressure for different clearances

stead-state pushrod stroke.

An estimation scheme for steady-state pushrod stroke that overcomes the problem of parameter sensitivity has been developed. The scheme assume a single break chamber operation, i.e., the treadle valve primary circuit meters compressed air to the front brake chamber and this configuration is shown in Figure 26. For the purpose of modeling and experimental simplification, such a layout was considered initially.

B. Energy based pushrod stroke estimation for a single brake chamber

The scheme is based on a model for brake chamber stored energy and transient pressure measurements. The brake chamber energy may be characterized by the pressure of air in the brake chamber (P_b) and the volume of brake chamber (V_b). Hence, a functional form of brake chamber energy is given by $E_b = P_b V_b$ and is

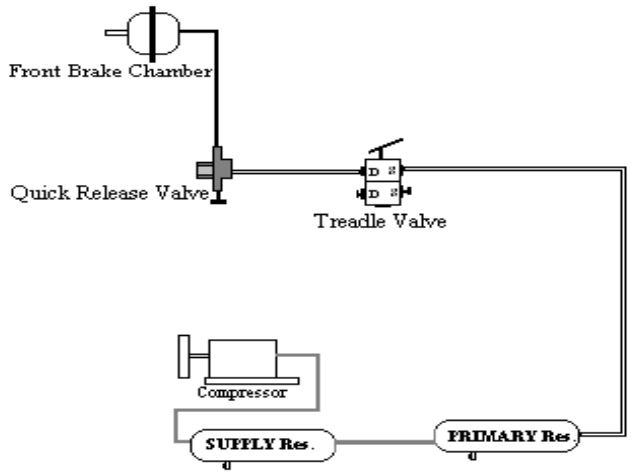

Fig. 26. Test setup configuration for pushrod stroke estimation - single brake chamber

related to the mass of air in the brake chamber through the constitutive equation of ideal gas law as follows:

$$E_b = m_{BC} R T_b, \tag{4.1}$$

where m_{BC} is mass of air in the brake chamber, R is the gas constant for air and T_b is the temperature of air in the brake chamber. It has been observed during experiments that the temperature changes are negligible. Hence, temperature is assumed to be constant and is same as the temperature of the surrounding air. Therefore, differentiating (4.1) with respect to time, we get:

$$\frac{d(E_b)}{dt} = \dot{m}_{BC} R T_b, \tag{4.2}$$

where $\dot{m}_{BC}$ is the mass flow rate of air entering the brake chamber. Also the constitutive equation for mass flow rate $\dot{m}_{BC}$ is given as follows [35]:

$$\dot{m}_{BC} = \rho A_p U, \tag{4.3}$$

where ρ is the density of air, A_p is the opening of the treadle valve, and U is the velocity of air flowing into the brake chamber. The density of air in the brake chamber

is related to the measured brake chamber pressure through following constitutive equation [34]:

$$\rho = \frac{P_m}{RT_b}, \tag{4.4}$$

where P_m is the measured brake chamber pressure. The area of the opening of treadle valve is estimated using the model developed by Subramanian et al. [33]. The input to the model is the treadle valve plunger displacement and the pressure measurements. A constitutive equation for U assuming isothermal flow of air is given as follows (Appendix B):

$$U = \sqrt{2RT_b log\left(\frac{P_0}{P_m}\right)}, \tag{4.5}$$

where P_0 is the supply pressure. Therefore substituting equations for ρ and U in (4.3), the equation for mass flow rate $\dot{m}_{BC}$ modifies as follows:

$$\dot{m}_{BC} = A_p \frac{P_m}{RT_b}\sqrt{2RT_b log\left(\frac{P_0}{P_m}\right)}. \tag{4.6}$$

The steady-state estimate of brake chamber energy, E_{b-ss} can be determined by numerically integrating (4.2) for the time interval for which steady-state pressure is achieved in the test setup. Also, the initial state of the brake chamber is assumed to be known i.e. $P_b(0) = P_{atm}$ (atmospheric pressure), $V_b(0) = V_i$ (V_i is the initial volume of the brake chamber). Therefore, the brake chamber energy at the start of braking is $E_b(0) = P_{atm}V_i$. The incoming mass flow rate $\dot{m}_{BC}$ is obtained from (4.6) for the given time interval. A linear relationship between volume of the brake chamber and the pushrod stroke has been assumed and is given as:

$$V_b(t) = V_i + A_b x_b(t), \tag{4.7}$$

where $x_b(t)$ is the pushrod stroke at any given time, $V_b(t)$ is the volume of brake chamber at the given time, V_i is the initial volume of the brake chamber and A_b is

the area of the brake chamber diaphragm. Hence, the steady-state pushrod stroke is computed using (4.7) as follows:

$$V_{b-ss} = \frac{E_{b-ss}}{P_{m-ss}}, \tag{4.8}$$

$$x_{b-ss} = \frac{V_{b-ss} - V_i}{A_b}, \tag{4.9}$$

where E_{b-ss} is steady-state estimate of E_b, P_{m-ss} is steady-state brake chamber pressure from measurements, V_{b-ss} is the estimated steady-state volume, x_{b-ss} is the estimated steady-state pushrod stroke.

Different pushrod strokes in the test setup are simulated by varying the clearance between the brake pad and the brake drum. The clearance can be changed by rotating the adjusting nut of the slack adjuster. Results obtained by the above scheme for different pushrod stroke settings at various supply pressures are summarized in Table IV.

Table IV. Pushrod stroke estimates for various supply pressures

Supply Pr. (psi/kPa)	Measured Stroke (X_b) (mm)	Estimated stroke (x_{b-ss}) (mm)	error (%) $= \frac{(X_b - x_{b-ss})}{X_b} \times 100$
90/722	49.27	51.14	-3.9
90/722	40.78	41.23	-1.01
90/722	26.6	22.19	16.6
80/653	37.5	40.98	-9.28
70/584	35.7	40.33	-12.9
70/584	52.14	45.33	13.06
60/515	33.33	38.46	-15.39
60/515	51.17	41.29	19.3

1. Treadle valve entry pressure and its effect on pushrod stroke estimation

The pressure measured (in the test setup) at the entry of the treadle valve's primary circuit was observed to vary during the pressure-rise phase, as shown in Figure 27. This may be specific to the test setup and might not happen in a real vehicle. However, the effect of ignoring this observation (assuming a constant supply pressure) on the brake chamber energy (E_b) predictions is shown in Figure 28 where E_b from experiments is computed using the measured brake chamber pressure and the corresponding pushrod stroke measurements from the test setup. A sinusoidal fit that relates the observed inlet pressure variation to the measured brake chamber pressure (P_m) and the rated supply pressure (P_0), is given as follows:

$$P_{in} = \begin{cases} P_0, \ P_m \geq P_0, \\ P_0 \left[A - B \sin \left(2\pi \left(\frac{P_m(t) - P_{atm}}{P_0 - P_{atm}} \right) \right) \right], \ P_m \in (P_{atm}, \ P_0), \end{cases} \tag{4.10}$$

where P_{in} is the pressure at the inlet of primary circuit of the treadle valve. The inlet pressure (P_{in}) computed using (4.10) and the inlet pressure measured in the test setup are compared and plotted in Figure 27. The brake chamber energy (E_b) predictions after substituting P_{in} for P_0 in (4.5) are shown in Figure 28. Clearly, the prediction of E_b is better with the substitution, which also leads to a better estimate of steady-state pushrod stroke.

C. Steady-state pushrod stroke estimate for the test setup configuration with two brake chambers

The estimation scheme in the previous section predicts the steady-state pushrod stroke for the data obtained from the test setup in a configuration wherein the primary delivery of the treadle valve is connected to a single brake chamber ("type 20").

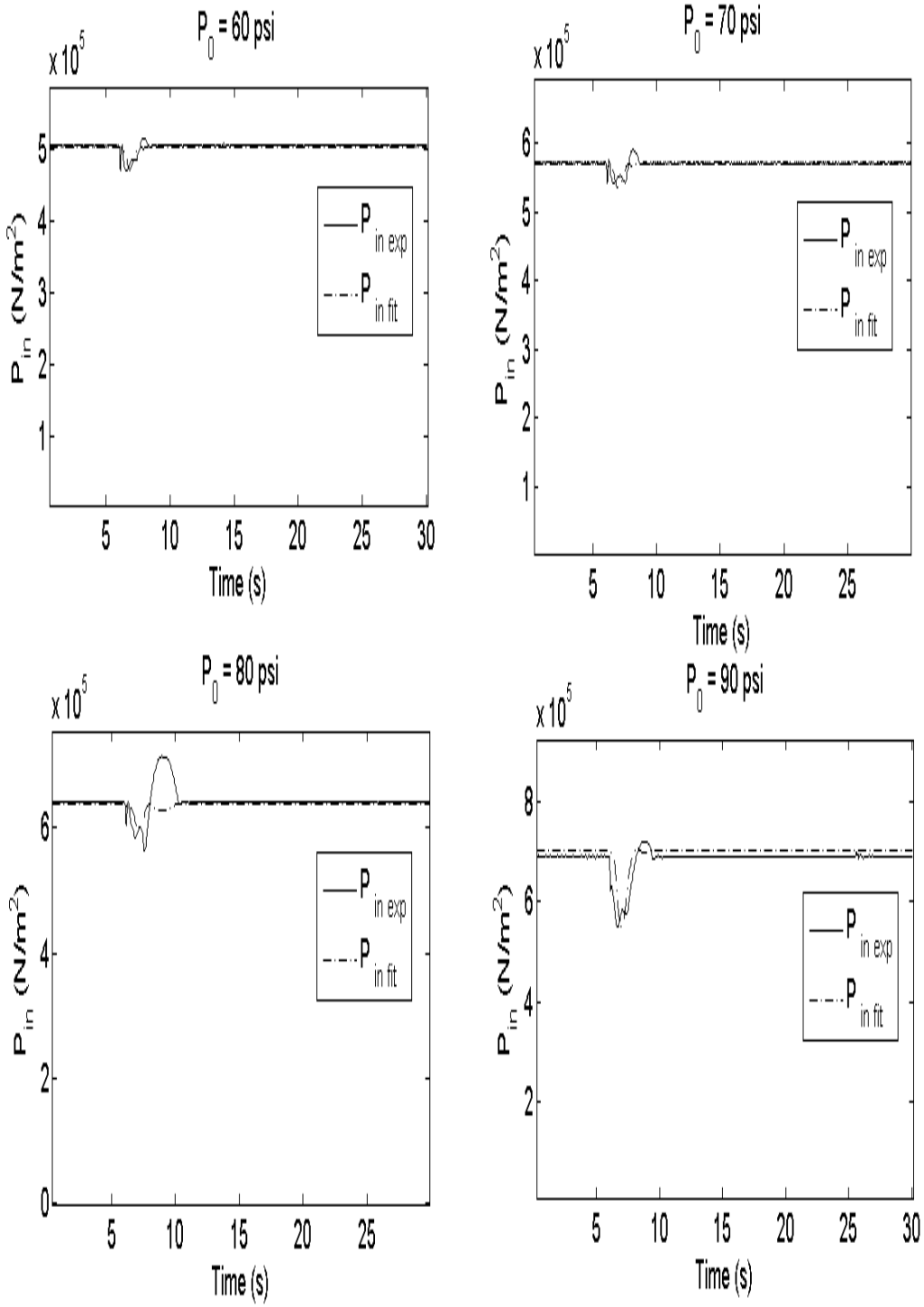

Fig. 27. Entry pressure in the treadle valve's primary circuit during braking

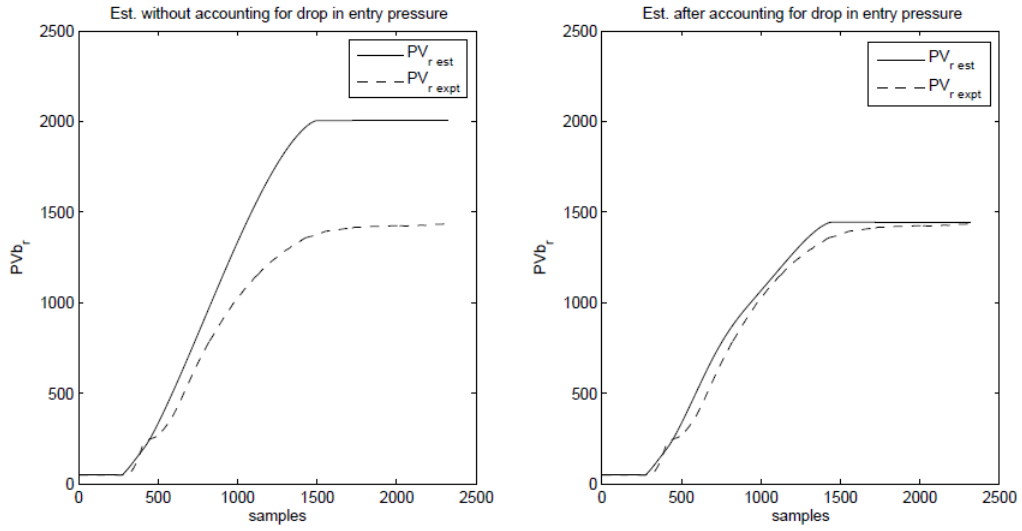

Fig. 28. Estimates of brake chamber energy without and with considering the drop in the entry pressure

For the scheme to be used in an actual vehicle and for the purposes of implementation and corroboration of the scheme, the test setup was configured to partially[2] resemble the brake system of an actual vehicle. In this configuration, the output of primary circuit of the treadle valve acts as the control input to the secondary valve and the relay valve, which meter the compressed air to the front and the rear brake chambers. Since the displacement transducers and the foundation brake assemblies are available only on the front axle in the test setup, a "type 30" brake chamber (rear brake chamber) has been fitted on one of the front wheels and a "type 20" brake chamber on the other, as shown in Figure 29.

[2]An actual configuration consists of an exact replica of the air brake system in a actual truck, including the foundation brake assembly linked to each brake chamber.

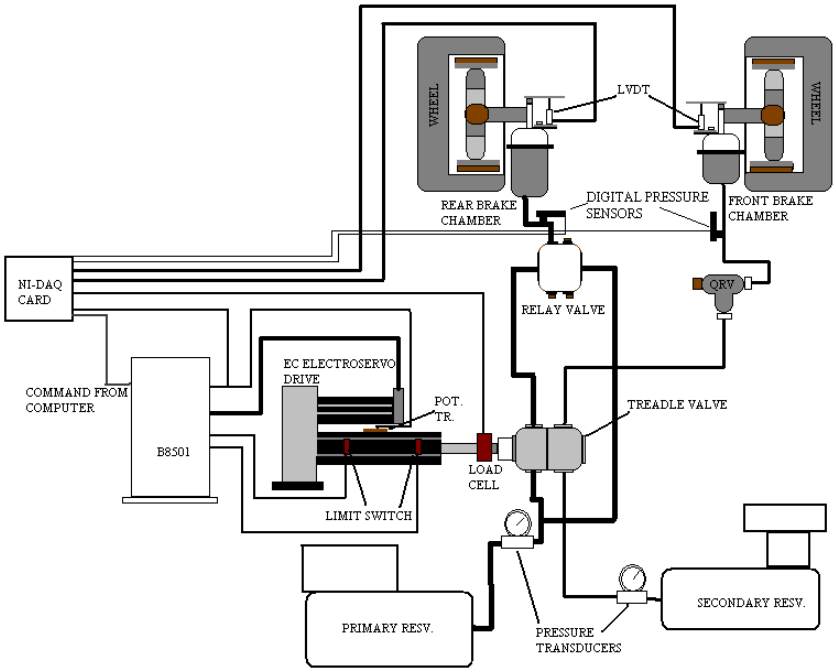

Fig. 29. Schematic for two chamber configuration of the test setup

1. Pressure transients in the delivery of the primary circuit

The area of treadle valve opening, in case of the single chamber configuration, has been estimated using the model for the treadle valve developed by Subramanian et al. [33]. The inputs to the model are the plunger displacement and pressure in the primary circuit of the treadle valve. In this case, the primary circuit's delivery pressure is same as the brake chamber pressure and is known from the measurements of the front brake chamber pressure.

However, in case of the configuration shown in Figure 29, the primary delivery is connected to the input of the relay valve. The pressure in the primary circuit, which act as an input to the secondary valve and the relay valve, is not measured and must be predicted. Pressure evolution in the primary circuit is governed by the motion of the primary piston, the secondary piston and the relay valve piston. Therefore,

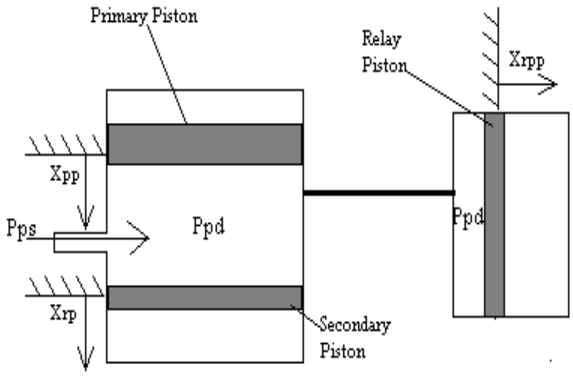

Fig. 30. Volume change in the primary circuit

volume the primary circuit is the total volume enclosed between the primary piston, the relay piston and the relay valve piston and changes according to the motion of all the three pistons, as shown in Figure 30. Also, the pressure transients in the primary circuit are similar to that of the air brake chamber wherein the volume changes due to the motion of pushrod.

Therefore, the governing equations for pressure transients in the primary circuit are as follows:

$$\begin{aligned} \dot{P}_p &= \frac{C_D A_{pv} \frac{P_p}{RT} U_E - P_p \dot{V}_p}{V_p}, \\ V_p &= V_{po} + A_{pe} x_{pp} + A_{se} x_{rp} + A_{re} x_{rpp}, \\ A_{pv} &= 2\pi r_{pp} (x_{pp} - x_{pt}). \end{aligned} \tag{4.11}$$

The nomenclature of parameters of (4.11) are given in Table V. x_{pp} and x_{rp} are determined using the treadle valve model by Subramanian et al. [33] and x_{rpp} is determined using the relay valve model by Natrajan et al. [46].

The experimental data that has been obtained for the corroboration of the scheme is for "full-brake" application, where in, the area of opening of the metering valve (secondary /relay) depends on the steady-state pressure in the primary circuit. The

Table V. Nomenclature of parameters/variables [33],[46], [47]

Parameter	Description	Value
x_{pp}	Displacement of the primary piston	m
x_{rp}	Displacement of the relay piston	m
x_{rpp}	Displacement of the relay valve piston	m
x_{pt}	Distance traveled by the primary piston before its contact with the primary valve	0.002273 m
P_p	Pressure in the primary circuit of the treadle valve	N/m^2
A_{pv}	Area of opening of primary valve	m^2
A_{pe}	Effective area of of the primary valve on the delivery side	0.002226 m^2
A_{se}	Effective area of of the relay piston on the high pressure side	0.003189 m^2
A_{re}	Effective area of of the relay valve piston on the high pressure side	0.0064 m^2
r_{pp}	radius of primary valve gasket	m
C_D	Coefficient of discharge of a nozzle	0.82
U_E	Velocity of air coming out of the primary valve	m/s
V_{po}	Initial volume enclosed between the primary piston and the primary valve	0.0001594 m^3
V_p	Volume of primary circuit at any given time instant	m^3

predictions of E_b using the predicted primary circuit pressure have been compared with E_b predictions using the measured primary circuit pressure in Figures 31 and 32.

2. Pushrod stroke estimates for the front and the rear brake chambers

The inputs to the models, that predict the openings of the secondary valve [33] and the relay valve [46], are the primary pressure obtained using (4.11), the pressure measurements of the front and the rear brake chambers and the treadle valve plunger displacement.

The governing equations for the steady-state pushrod stroke estimation of the

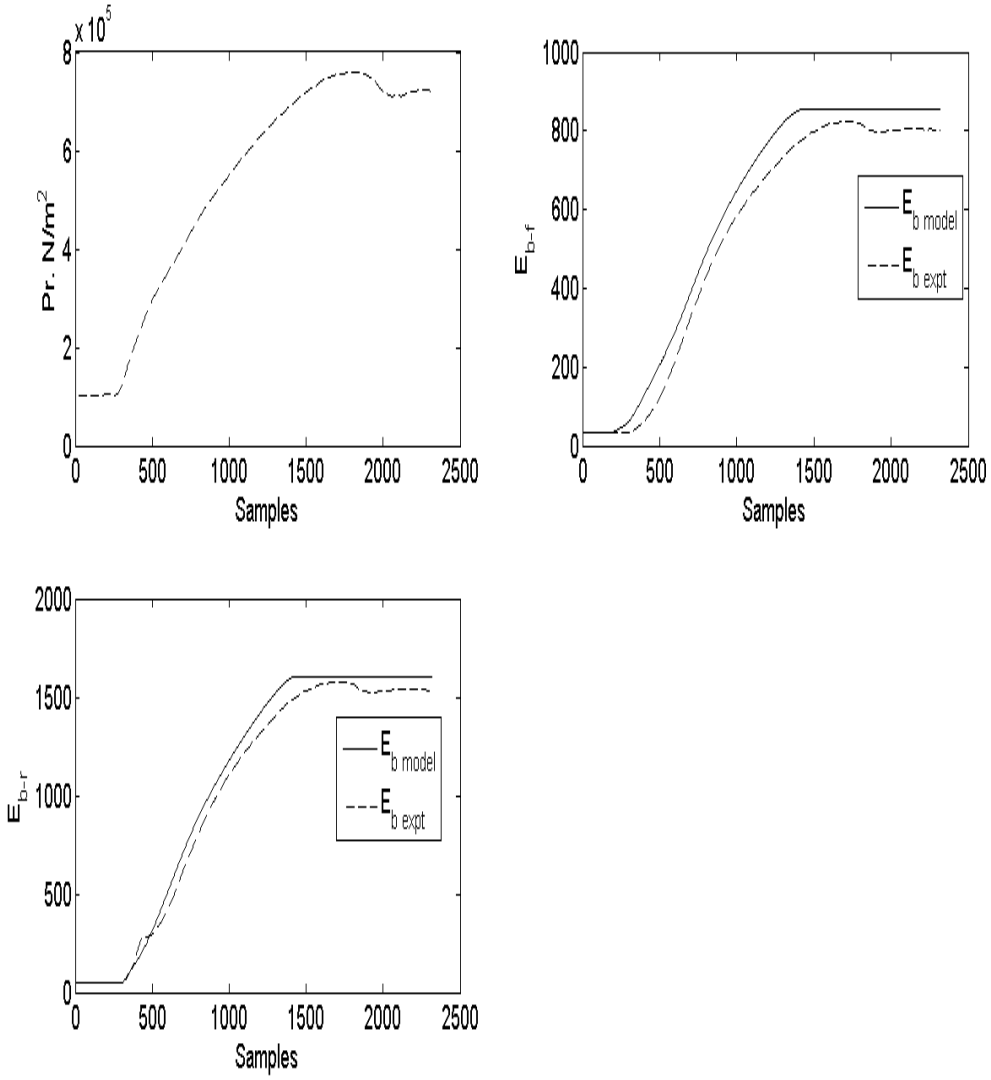

Fig. 31. Estimate of E_b for the front and the rear brake chamber using measured primary circuit pressure

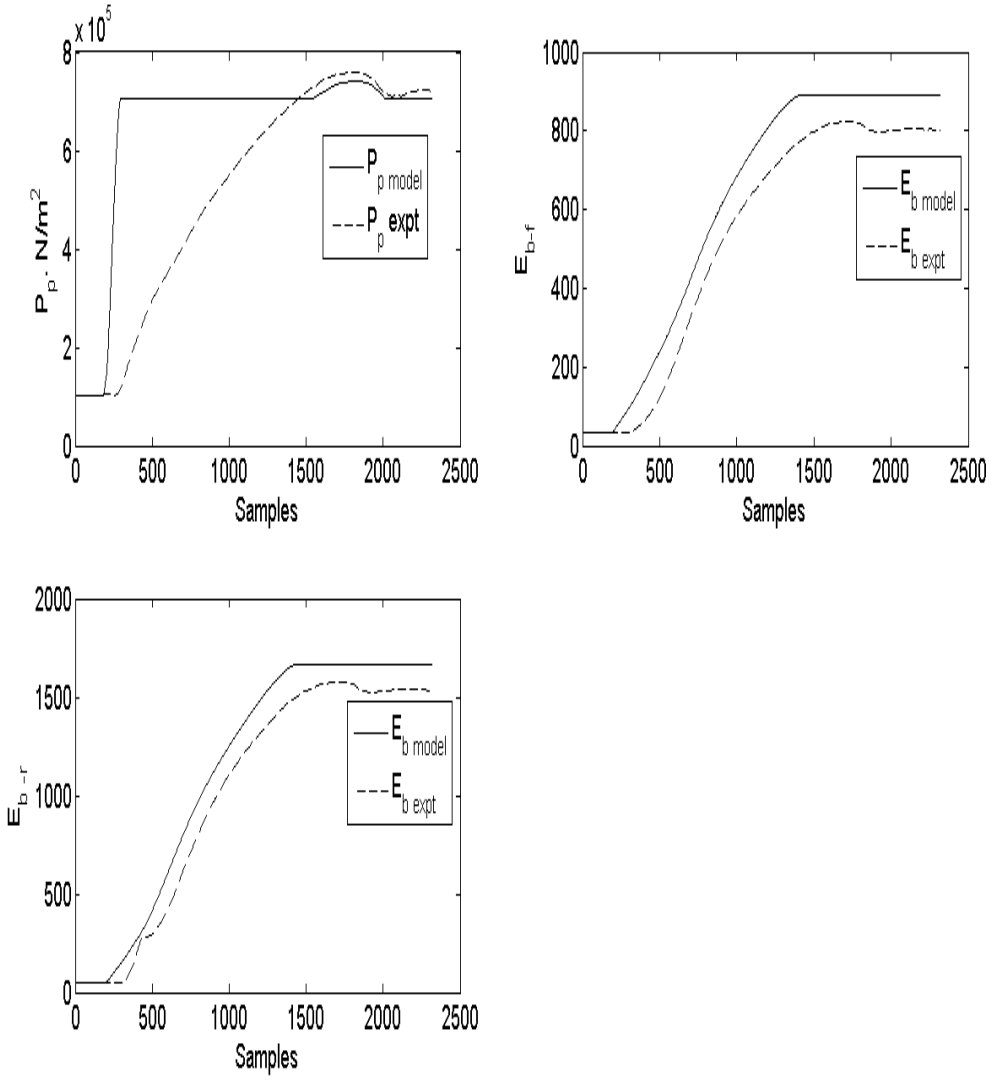

Fig. 32. Estimate of E_b for the front and the rear brake chamber using the predicted primary circuit pressure

front brake chamber are as follows:

$$\begin{aligned} \frac{d(E_{b-f})}{dt} &= \dot{m}_{BC-f} R T_b, \\ \dot{m}_{BC-f} &= A_{sv} \frac{P_{sdm}}{RT_b} \sqrt{2RT_b log\left(\frac{P_{in}}{P_{sdm}}\right)}, \\ A_{sv} &= 2\pi r_{sv}(x_{rp} - x_{st}), \end{aligned} \tag{4.12}$$

where E_{b-f} is the front brake chamber energy, A_{sv} is the area of opening of the secondary valve, $\dot{m}_{BC-f}$ is the mass flow rate of air into the front brake chamber and depends on the brake chamber pressure and the area of opening of the secondary valve and P_{sdm} is the measured pressure in the front brake chamber. Figures 31 and 32 compare the estimated brake chamber energy (E_b) with E_b computed using the measured brake chamber pressure and the corresponding pushrod stroke measurements. The relationship between volume of the brake chamber and the pushrod stroke is of the following form:

$$V_{b-f}(t) = V_{i-f} + A_{b-f} x_{b-f}(t), \tag{4.13}$$

where $x_{b-f}(t)$ is the pushrod stroke of the front brake chamber at any given time , $V_{b-f}(t)$ is the volume of the front brake chamber at the given time, V_{i-f} is the initial volume of the front brake chamber (Type 20) and A_{b-f} is the area of the front brake chamber's diaphragm. Hence, the steady-state pushrod stroke is computed using 4.13 as follows.

$$\begin{aligned} V_{bf-ss} &= \frac{E_{bf-ss}}{P_{sdm-ss}}, \\ x_{bf-ss} &= \frac{V_{bf-ss} - V_{i-f}}{A_{b-f}}, \end{aligned} \tag{4.14}$$

where E_{bf-ss} is steady-state estimate of E_{b-f}, P_{sdm-ss} is steady-state front brake chamber pressure from measurements, V_{bf-ss} is the steady-state volume, x_{bf-ss} is

steady-state pushrod stroke of the front brake chamber. Equations similar to the front brake chamber have been used to estimate the steady-state pushrod stroke of the rear brake chamber.

The steady-state pushrod stroke estimated using the scheme, for the front and the rear brake chambers and for various settings of the slack adjuster nut in the experimental setup, are listed alongwith the corresponding steady-state pushrod stroke measurements in Table VI. The experiments for other supply pressure were not performed since the inspection for the out-of-adjustment of pushrod are standardized for the supply pressure of 90 psi.

Table VI. Pushrod stroke estimates for 90 psi supply for front and rear brake chambers

Brake Chamber	Measured Stroke (X_b) (mm)	Estimated stroke (x_{b-ss}) (mm)	error (%) $= \frac{(X_b - x_{b-ss})}{X_b} \times 100$
Front	37.97	42.68	-12.40
	54.5	49.7	8.88
Rear	66.39	69.52	-4.75
	68.26	60.12	11.92

CHAPTER V

ESTIMATION OF PARAMETERS OF A CLASS OF HYBRID SYSTEMS

In this chapter, the problem of parameter estimation of a class of hybrid systems that are frequently encountered in systems with accumulation of fluids such as the air brake system, has been addressed.

A. The problem of parameter estimation

The equations governing the pressure of air in the brake chamber depend on the position and velocity of the pushrod (refer [33]). The evolution of displacement depends on the pressure acting on the pushrod. The pressure of compressed air and its derivatives and the displacement of pushrod and its derivative form two sets of states with the pressure being the measured variable or the output of the air brake system. Pressure acting on the pushrod causes motion and the mode in which the system operates depends on the displacement of the pushrod. The motion of the pushrod also depends on the clearance between the brake pad and the drum which can vary due to a variety of factors (refer Chapter I). For such applications, characterizing mode-to-mode transition parameters requires a lot of constitutive assumptions. Also, it can be difficult to calibrate the parameters associated with the constitutive assumptions. We therefore treat the air brake system as a hybrid system where the parameter governing the transition from one mode to another (clearance between the brake pads and the drum) is not known exactly. Therefore, the problem of estimation is as follows: Suppose the pressure of the air brake system were to be measured and

---

*Part of this chapter is reprinted with permission from "Identification and Estimation of Parameters Defining a Class of Hybrid Systems" by S. Dhar, S. Darbha and K.R. Rajagopal, 2010, *Nonlinear Analysis: Hybrid Systems*, accepted.

that the motion of the pushrod is not measured. Is it possible to estimate the final displacement of the pushrod *without knowing the parameters (clearance)* that govern the system to transition from one mode to another?

B. An approach to solve the problem of parameter estimation

The approach to the parameter estimation problem is as follows: Suppose the pressure measurements in the air brake system corresponding to full application of the brake pedal for a duration of T seconds are available. Suppose one were to now disconnect the pushrod from the springs to obtain a modified nonhybrid system. This modified system consists only of a piston cylinder arrangement with compressed air from the reservoir entering cylinder as in a real air brake system. Suppose we were to control the motion of piston and springs using force on the piston. What should the controlled force of the piston be so that the evolution of pressure in the modified system is the exactly same as the measured pressure? Clearly, one can obtain a non-smooth state feedback control law which mimics the forces exerted by the springs and the pushrod and the evolution of pressure in the modified as well as the hybrid system will be identical. The control scheme will require the knowledge of parameters governing the mode-to-mode transitions of the hybrid system. We circumvent this problem by treating the measured pressure from the hybrid system as the desired pressure to be tracked by the modified system. We seek to determine a smooth nonlinear feedback control scheme that ensures the error between the pressure in the modified system and the measured pressure goes to zero. The feedback control input will, in general, be a nonlinear function of the states of the modified system, the pressure error (difference between the pressure of the modified system and the measured pressure) as well as its derivatives and derivatives of the measured pressure, which may be

assumed to be known for this application. Correspondingly, one can obtain a governing differential equation for the motion of the piston which represents the internal dynamics,which can be assumed to be stable from physical considerations. Hence, the final displacement of the piston can be estimated by integrating this differential equation while circumventing the hybrid nature of the system. One can subsequently estimate the mode transition parameters through the computation of net force acting on the piston.

C. Problem formulation

A class of hybrid systems, motivated by the air brake system, is considered with two sets of states: a set describing the accumulation process such as the pressure, y and its first $r-1$ derivatives with respect to time, $y^{(1)}, y^{(2)}, \ldots, y^{(r-1)}$ and the other set describes the motion with the displacement, z of the piston and its first $l-1$ derivatives with respect to time, $z^{(1)}, z^{(2)}, \ldots, z^{(l-1)}$. The l^{th} derivative of the displacement variable affects the evolution of the r^{th} derivative of the accumulation variable and the l^{th} derivative of the motion is affected by the hybrid nature of the system, which depends not only on the displacement, z, but may also depend on the accumulation variable y and its derivatives. This is a very common situation in multi-stage devices where the stage is determined by the displacement of a mass or deflection of a spring. For the sake of notation, Y is the ordered tuple $(y, y^{(1)}, \ldots, y^{(r-1)})$ and Z is the ordered tuple $(z, z^{(1)}, z^{(2)}, \ldots, z^{(l-1)})$. The governing equations may be described through appropriate smooth functions $f_1(Y,Z)$, $f_0(Y,Z)$ and possibly a non-smooth function $\phi(Y,Z)$ as:

$$y^{(r)} = f_1(Y,Z) + f_0(Y,Z)z^{(l)}, \tag{5.1}$$

$$z^{(l)} = \phi(Y,Z). \tag{5.2}$$

To describe the sequential nature of the hybrid system, let $z_1^*, z_2^*, \ldots, z_m^*$ denote a set of m real numbers in ascending order. Let $\phi_i(Y, Z),\ i = 1, \ldots, m$ denote m smooth non-linear functions. For each $i = 1, \ldots, m$, let $\zeta_i(Y, z)$ denote a smooth function which defines a transition for the hybrid system as follows:

1. The inequality $\zeta_1(Y, z) < z_1^*$ implies that and is implied by the system being in the first mode.

2. The inequalities $\zeta_i(Y, z) \geq z_i^*$, $\zeta_{i+1}(Y, z) < z_{i+1}^*$ hold if and only if, the system is in $(i+1)^{th}$ mode for $i \geq 1$ and $i \leq m-2$.

3. $\zeta_m(Y, z) \geq z_m^*$ holds if and only if, the system is in m^{th} mode.

The response of the nonlinear hybrid system (5.1) is assumed to be stable. This is a reasonable assumption for the problem of air brakes or any other passive mechanical system.

Since this is a problem of fault diagnosis, one may run the estimation scheme after the measurement has been made over the interval $[0, T]$. For that reason, it is assumed that the measurement can be processed and any noise, if present, can be completely removed. Usually pressure measurement is reasonably clean and can be filtered of any noise. Therefore, one may assume that not only the variable $y(t)$ but also its derivatives are available. From hereon, $y_m(t)$ refers to the measured pressure in the air brake system.

The problem is as follows: Suppose $z_1^*, \ldots, z_m^*$ are not known. Is it possible to estimate $z(T)$ from the measurement of $y_m(t)$ on the specified interval $[0, T]$? One may assume that the initial conditions are known exactly.

D. Estimation scheme

The problem of estimation can be converted to a problem of nonlinear control design by circumventing the hybrid nature of the system. Essentially, we can ask the following question: Suppose the output has been measured for T seconds. Further, suppose the l^{th} time derivative of the displacement variable, z, were to be specified so that the pressure, y, tracks the measured pressure, $y_m(t),\ t \in [0, T]$. In other words, if were to consider the following nonlinear system:

$$y^{(r)} = f_1(Y, Z) + f_0(Y, Z)u, \tag{5.3}$$

$$z^{(l)} = u, \tag{5.4}$$

the question we ask is whether u can be chosen so as to ensure that y tracks the measured output $y_m(t)$. Clearly, $u = \phi(Y, Z)$ accomplishes what we seek; however, such a feedback law has a number of unknown quantities $z_1^*, z_2^*, \ldots, z_m^*$, and hence may not be useful for the purpose of estimation.

Following assumptions have been made regarding the proposed estimation scheme:

1. Since there is a feedback law $u = \phi(Y, Z)$ that results in the output, $y(t)$, of the nonlinear hybrid system (5.24) the same as the measured output $y_m(t)$, one may assume that "internal dynamics" obtained by constraining $y(t)$ to be identical to $y_m(t)$ is "stable".

2. The term $f_0(Y, Z) \neq 0$, so that we may derive a feedback linearizing control law. This can be a potentially limiting assumption. However, for the mechanical systems we have in mind and as the examples show later in this paper, this assumption is not an unreasonable one.

Let $k_1, \ldots, k_r$ be real positive numbers such that the polynomial $\Delta(s) = s^r +$

$k_1 s^{r-1} + \ldots + k_r$ is Hurwitz, i.e., all the roots of this polynomial have a negative real part. Then, one may easily see that the following control law ensures the desired result for $y(t)$ tracking $y_m(t)$ ([48]- [50]):

$$u = \frac{1}{f_0(Y,Z)}[y_m^{(r)}(t) - k_1(y^{(r-1)}(t) - y_m^{(r-1)}(t)) - k_2(y^{(r-2)}(t) - y_m^{(r-2)}(t)) \\ - \cdots - k_r(y(t) - y_m(t)) - f_1(Y,Z)]. \quad (5.5)$$

If the output, $y(t)$, were to track $y_m(t)$ exactly, then, we have the following evolution equation for z:

$$z^{(l)} = \frac{(y_m^{(r)}(t) - f_1(Y,Z))}{f_0(Y,Z)}. \quad (5.6)$$

The estimation scheme involves numerically integrating the last equation (5.36) on the interval $[0,T]$ by setting $y(t)$ to be identical to $y_m(t)$. Therefore, Y in the equation (5.36) is known. Since the initial condition for z is assumed known, this equation can be numerically integrated to obtain $z(T)$.

From equation (5.36), one may estimate the mode the system is in at any instant of time $t \in [0,T]$ by comparing u with $\phi_i(Y,Z)$ for each $i = 1, \ldots, m$ and determining the argument i for which $|\phi_i(Y,Z) - u|$ is a minimum for a duration of time $\Delta > 0$ and smaller than the duration of time spent by the hybrid system in each mode.

E. Illustrative examples

The estimator design for the class of hybrid systems, discussed previously, has been illustrated through examples. In the first case, a pneumatic system similar to the

pneumatic system found in air brakes has been considered [45] and is given as follows:

$$\begin{aligned} \dot{P}_b &= \frac{A_p P_b \sqrt{2RTlog\left(\frac{P_o}{P_b}\right)} - A_b \dot{x_b} P_b}{A_b x_b + V_{o1}}, \\ m\ddot{x_b} &= \begin{cases} (P_b - P_{atm})A_b - C_1\dot{x_b} - K_1 x_b, \ P_b < P_{th}, \\ (P_b - P_{atm})A_b - C_2\dot{x_b} - K_2 x_b, \ P_{th} \leq P_b < P_{ct}, \\ (P_b - P_{atm})A_b - C_3\dot{x_b} - K_3 x_b, \ P_b \geq P_{ct}, \end{cases} \end{aligned} \tag{5.7}$$

where nomenclature of the system parameters and variables is given in Table VII:

Table VII. Nomenclature of parameters/variables used

Parameter/Variable	Description	value
R	Gas constant for air	287 J/kgK
T	Ambient temperature	293 K
P_b	Brake chamber pressure	N/m^2
P_o	Supply pressure	7.22×10^5 N/m^2
A_p	Area of treadle valve opening	3.1669×10^{-5} m^2
x_b	Pushrod stroke	m
P_{atm}	Atmospheric pressure	101325 N/m^2
P_{th}	Push-out pressure	1.4273×10^5 N/m^2
P_{ct}	Contact pressure	$2.3926 \times 10^5 N/m^2$
$z_{clearance}$	Brake pad and brake drum clearance	0.6 mm
m	Mass of pushrod and diaphragm	5 kg
A_b	Area of brake chamber diaphragm	0.0129 m^2
V_{o1}	Initial volume of brake chamber	0.00032774 m^3
K_1	Spring constant for Mode-I	2.1972×10^3 N/m
K_2	Spring constant for Mode-II	4.3944×10^3 N/m
K_3	Spring constant for Mode-III	6.5916×10^3 N/m
C_1	Damping coefficient for Mode-I	20.96 Ns/m
C_2	Damping coefficient for Mode-II	29.64 Ns/m
C_3	Damping coefficient for Mode-III	36.31 Ns/m

The states of the pneumatic system are pressure (P_b), pushrod stroke (x_b) and velocity of the pushrod ($\dot{x_b}$). Let us denote P_b by y, x_b by z_1 and $\dot{x_b}$ by z_2. With the

change of variables, the above equations may be expressed as:

$$\begin{aligned}
\dot{y} &= \frac{A_p y\sqrt{2RTlog\left(\frac{P_o}{y}\right)} - A_b z_2 y}{A_b z_1 + V_{o1}}, \\
\dot{z_1} &= z_2, \\
m\dot{z_2} &= \begin{cases} (y - P_{atm})A_b - C_1 z_2 - K_1 z_1, \ y < P_{th}, \\ (y - P_{atm})A_b - C_2 z_2 - K_2 z_1, \ y \geq P_{th}, \ z_1 < z_{clearance}, \\ (y - P_{atm})A_b - C_3 z_2 - K_3 z_1, \ z_1 \geq z_{clearance}, \end{cases} \\
y_m &= y, \qquad (5.8)
\end{aligned}$$

where y_m is the (measured) output of the system during $[0, T]$. A typical simulated response of the pneumatic system (5.7) for the parameter values listed in Table VII is shown in Figure 33.

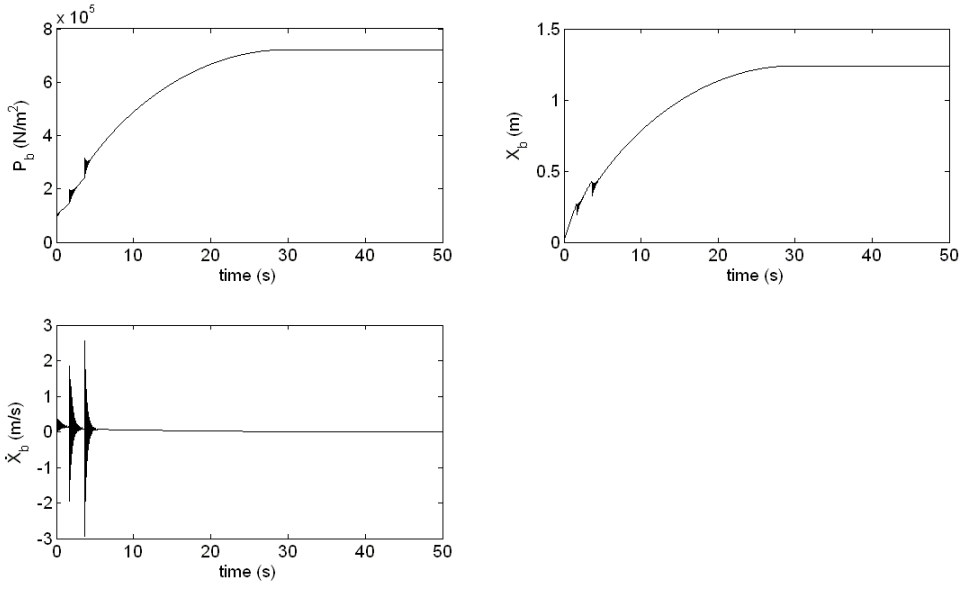

Fig. 33. Simulated response of the hybrid system

1. Estimation of the parameters of the hybrid system

The nonlinear system for the purpose of steady-state parameter estimation, by first neglecting the mass m of the piston is as follows. As explained earlier, a modified system is constructed where the pushrod is disconnected from the piston. Since the inertia of the piston is neglected, velocity of the piston may be thought of as a control input which may be specified arbitrarily. Correspondingly, the governing equations for the hybrid and the modified system may be expressed as:

$$\begin{aligned}
\dot{y} &= \frac{A_p y\sqrt{2RTlog\left(\frac{P_o}{y}\right)} - A_b\dot{z}_1 y}{A_b z_1 + V_{o1}}, \\
\dot{z_1} &= \begin{cases} \frac{1}{C_1}\left[(y - P_{atm})A_b - K_1 z_1\right], \ y < P_{th}, \\ \frac{1}{C_2}\left[(y - P_{atm})A_b - K_2 z_1\right], \ y \geq P_{th}, \ z_1 < z_{clearance}, \\ \frac{1}{C_3}\left[(y - P_{atm})A_b - K_3 z_1\right], \ z_1 \geq z_{clearance}, \end{cases} \\
y_m &= y. \qquad (5.9)
\end{aligned}$$

The non-hybrid system for estimation of the steady-state parameter $z_1(T)$ of the hybrid system (5.9) is therefore:

$$\begin{aligned}
\dot{y} &= \frac{A_p y\sqrt{2RTlog\left(\frac{P_o}{y}\right)} - A_b u_v y}{A_b z_1 + V_{o1}}, \\
\dot{z}_1 &= u_v, \qquad (5.10)
\end{aligned}$$

where u_v is the control input. The controller u_v for (5.10)is designed such that $y(t)$ exactly matches $y_m(t)$ on the interval $[0, T]$. The measured output of the hybrid system (5.9) may be assumed to be sufficiently smooth, i.e. $\dot{y}_m$, $\ddot{y}_m$ are available.

From (5.10), it can see that the control input u_v affects the first time derivative of the output. If the right-hand side of the equation for $\dot{y}$ in (5.10) were to be equal

to $\dot{y}_m - k_1(y - y_m)$ for some $k_1 > 0$, then the error $e(t) := y - y_m$ will evolve according to the following differential equation:

$$\dot{e} + k_1 e = 0.$$

In other words, the error will converge to zero exponentially and the rate of convergence is governed by k_1 which may be chosen so that the error response is fast enough for the identification to be performed in the interval $[0, T]$. The control input u_v that ensures that the right-hand side of the equation for $\dot{y}$ in (5.10) is equal to $\dot{y}_m - k_1(y - y_m)$ is given by:

$$u_v = \frac{1}{A_b y}\left[-(\dot{y}_m - k_1(y - y_m))(A_b z_1 + V_{o1}) + \phi(y)\right], \tag{5.11}$$

where $\phi(y) = A_p y\sqrt{2RTlog\left(\frac{P_o}{y}\right)}$ and since y is strictly positive on the interval $[0, T]$, $A_p y \neq 0$. However, for exact tracking, $y(t) = y_m(t)$ for $t \in [0, T]$. Therefore, replacing y with y_m in (5.10) and substituting for u_v from (5.11), the estimator for z_1 is as follows:

$$\begin{aligned} \dot{\hat{z}}_1 &= \frac{1}{A_b y_m}\left[-\dot{y}_m(A_b \hat{z}_1 + V_{o1}) + \phi(y_m)\right], \\ \hat{z}_1(0) &= 0. \end{aligned} \tag{5.12}$$

Simulations, in Figure 34, show that in steady-state $\hat{z}_1$ tends to z_1 of the hybrid system.

In cases where the mass m of the piston is significant and cannot be neglected, the derivation of control input is more complicated and such a case has been considered

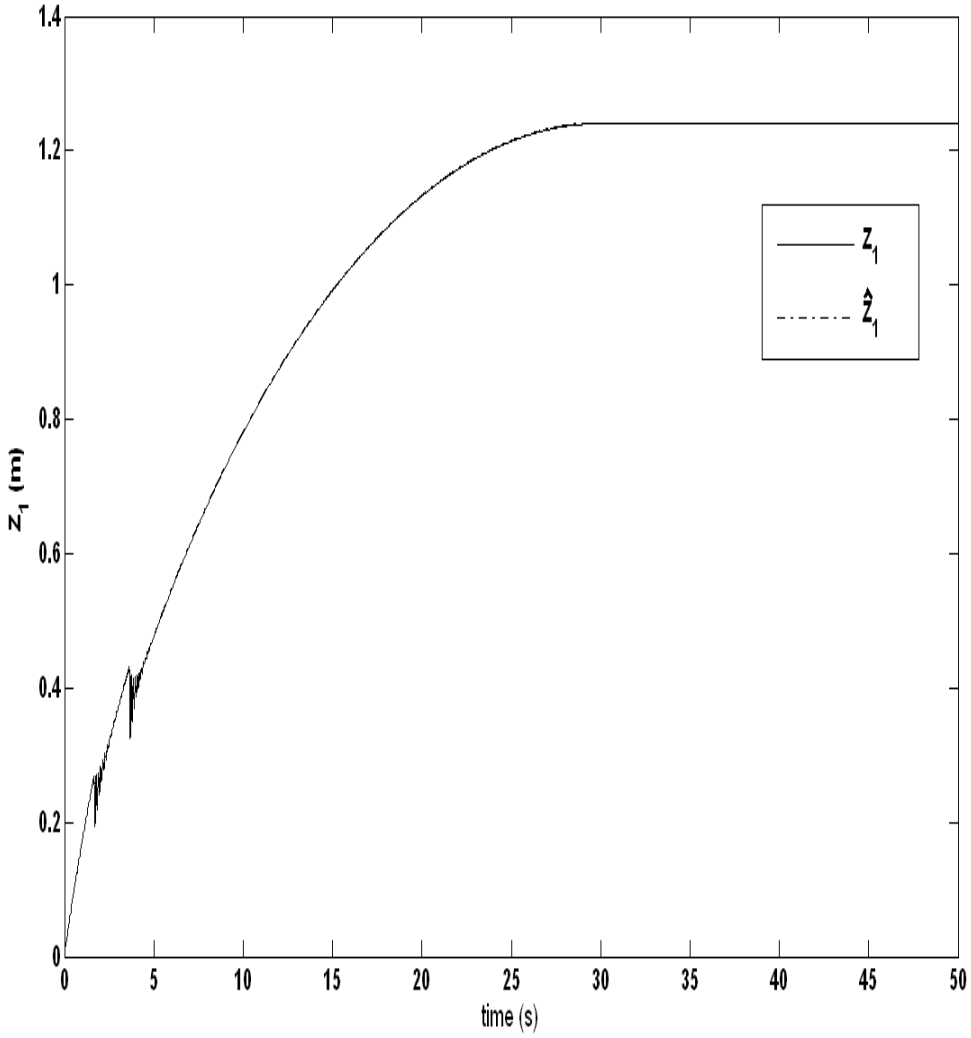

Fig. 34. Steady-state estimate of z_1 of the pneumatic hybrid system with massless piston

now:

$$\begin{aligned} \dot{y} &= \frac{A_p y\sqrt{2RTlog\left(\frac{P_o}{y}\right)} - A_b z_2 y}{A_b z_1 + V_{o1}}, \\ \dot{z}_1 &= z_2, \\ \dot{z}_2 &= u_a, \end{aligned} \tag{5.13}$$

where u_a is the force per unit mass that can be applied on the piston. The controller u_a is designed, such that $y(t)$ exactly matches $y_m(t)$ on the interval $[0, T]$. Also, y_m, $\dot{y}_m$ and $\ddot{y}_m$ are assumed to be available a priori. By taking successive time derivatives of y, one can see that the input u_a affects the second time derivative of the output y:

$$\begin{aligned} \dot{y} &= \psi(y, z_1, z_2), \\ \ddot{y} &= \frac{\partial \psi}{\partial y}\dot{y} + \frac{\partial \psi}{\partial z_1}\dot{z}_1 + \frac{\partial \psi}{\partial z_2}u_a, \end{aligned} \tag{5.14}$$

where $\psi(y, z_1, z_2) = \frac{A_p y\sqrt{2RTlog\left(\frac{P_o}{y}\right)} - A_b z_2 y}{A_b z_1 + V_{o1}}$. Therefore, if the right-hand side of the equation for $\ddot{y}$ were made to be equal to $\ddot{y}_m - k_1(\dot{y} - \dot{y}_m) - k_2(y - y_m)$ in (5.14), the following error differential equation is obtained:

$$\ddot{e} + k_1\dot{e} + k_2 e = 0.$$

The characteristic polynomial for the error evolution equation above is:

$$\Delta(s) = s^2 + k_1 s + k_2,$$

where $k_1 > 0$ and $k_2 > 0$ may be chosen to ensure $\Delta(s)$ to be Hurwitz. Correspondingly e and $\dot{e}$ converge to zero exponentially. Therefore, the controller u_a that ensures $\ddot{y} = \ddot{y}_m - k_1(\dot{y} - \dot{y}_m) - k_2(y - y_m)$ in (5.14), is given by:

$$u_a = \frac{1}{\frac{\partial \psi}{\partial z_2}}\left[\ddot{y}_m - \frac{\partial \psi}{\partial y}\psi - \frac{\partial \psi}{\partial z_1}z_2 - k_1(\psi - \dot{y}_m) - k_2(y_- y_m)\right]. \tag{5.15}$$

Since, the output y is constrained to follow y_m exactly, (5.15) modifies as follows:

$$u_a = \frac{1}{\acute{\psi}_{z_2}(y_m, z_1, z_2)}[\ddot{y}_m - \acute{\psi}_y(y_m, z_1, z_2)\psi(y_m, z_1, z_2) - \acute{\psi}_{z_1}(y_m, z_1, z_2)z_2], \quad (5.16)$$

where $\acute{\psi}_{()} = \frac{\partial \psi}{\partial ()}$. Since $y_m \neq 0$, $V_{o1} \neq 0$ and $z_1 \geq 0$ on the interval $[0, T]$, $\acute{\psi}_{z_2}(y_m, z_1, z_2) = \frac{A_b y_m}{A_b z_1 + V_{o1}} \neq 0$ on this interval. Therefore, the estimator for z_1 and z_2 is given as follows:

$$\begin{aligned}
\dot{\hat{z}}_1 &= \frac{1}{A_b y_m}\left[A_p y_m \sqrt{2RTlog\left(\frac{P_o}{y_m}\right)} - \dot{y}_m(A_b \hat{z}_1 + V_{o1})\right], \\
\dot{\hat{z}}_2 &= \hat{u}_a, \\
\hat{z}_1(0) &= 0, \\
\hat{z}_2(0) &= 0, \qquad (5.17)
\end{aligned}$$

where $\hat{u}_a = u_a(y_m, \hat{z}_1, \hat{z}_2)$. Equation (5.17) may be numerically integrated using the given initial conditions to estimate the steady-state parameters of the hybrid system. The simulations are shown in Figure 35.

2. Estimator design for a mechanical hybrid system

A mechanical hybrid system for which the steady-state estimator is designed is shown in Figure 36. The governing differential equations for this system are as follows:

$$\begin{aligned}
\dot{y} &= y_v, \\
M_1 \dot{y}_v &= -K_{12} y - C_{12} y_v + K_2 z + C_2 z_v, \\
\dot{z} &= z_v, \\
M_2 \dot{z}_v &= \begin{cases} -K_2(z - y) - C_2(z_v - y_v) + F, & z < L, \\ -C_2(z_v - y_v) - K_2(z - y) - K_3(z - L) - C_3 z_v + F, & z \geq L, \end{cases} \\
y_m &= y, \qquad (5.18)
\end{aligned}$$

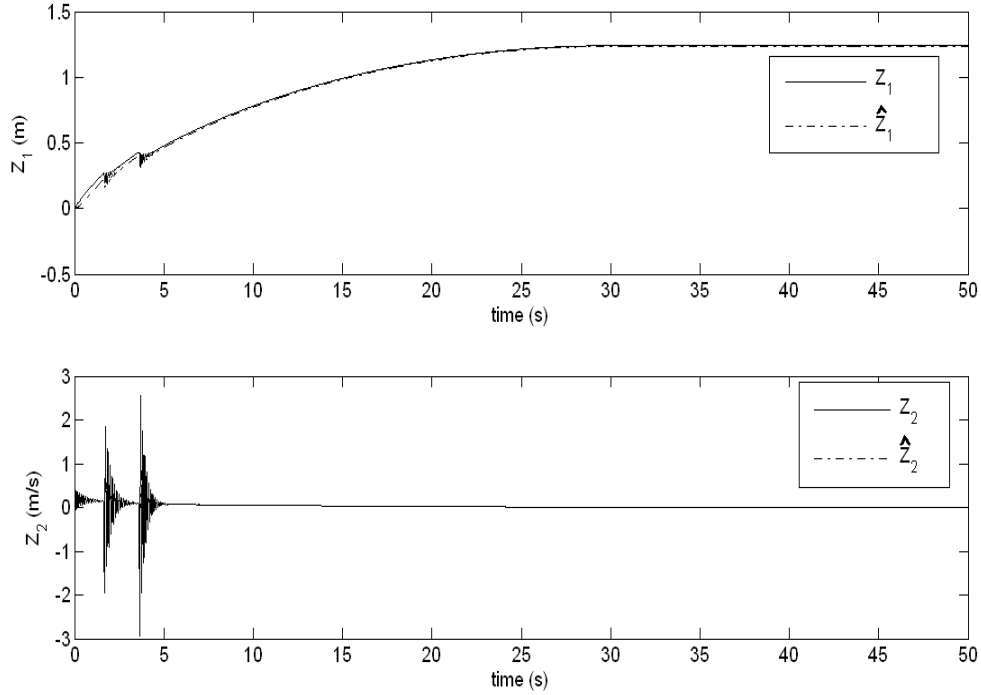

Fig. 35. Steady-state estimates of z_1 and z_2 of the pneumatic hybrid system

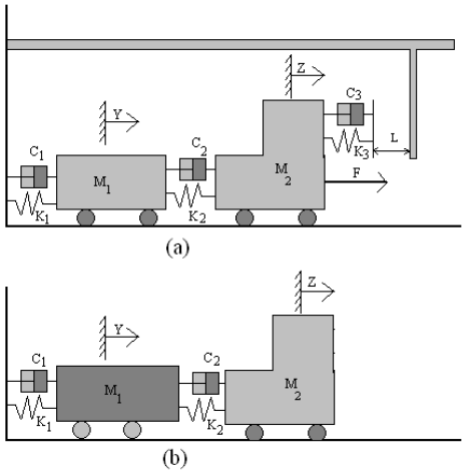

Fig. 36. (a) Mechanical hybrid system, (b) non-hybrid counterpart

where $K_{12} = K_1 + K_2$, $C_{12} = C_1 + C_2$, y_m is the measured output of the system, (y, y_v) are the displacement and velocity of M_1 and (z, z_v) are that of M_2. The parameters that are to be estimated are z and z_v of M_2. A typical response of the above system is shown in Figure 37. The system for steady-state parameter estimation is as shown

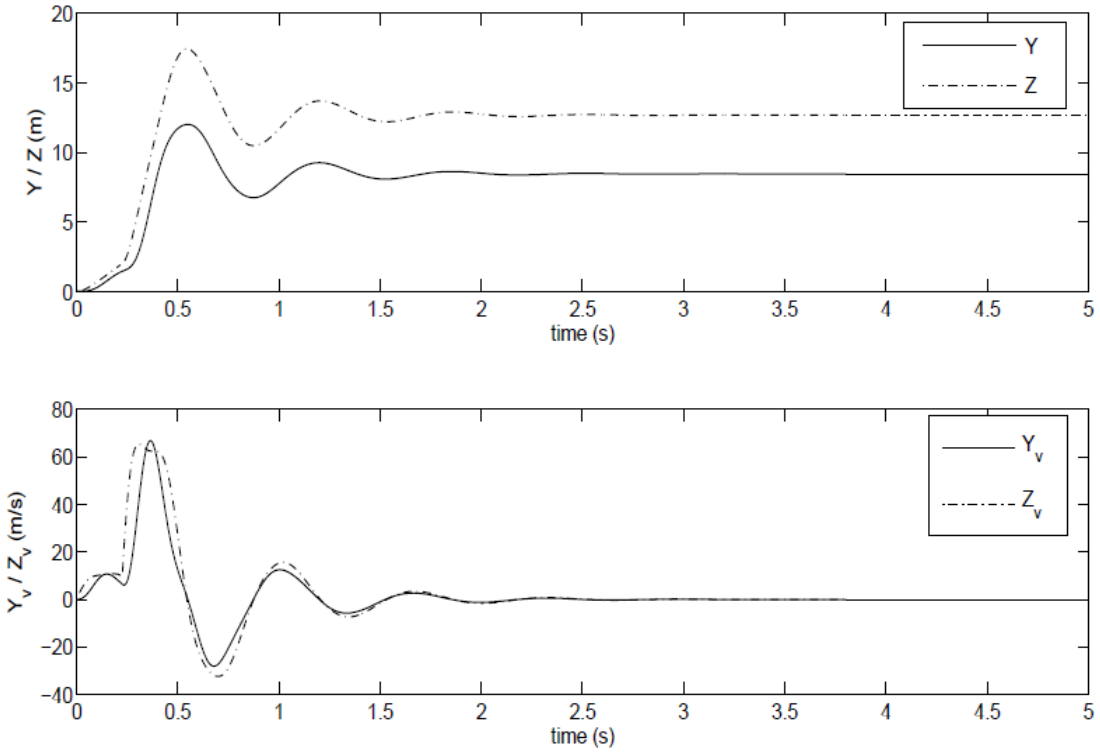

Fig. 37. Simulated response of the mechanical hybrid system

in Figure 36 and its governing equations are as follows:

$$\begin{aligned} \dot{y} &= y_v, \\ M_1 \dot{y}_v &= -K_{12} y - C_{12} y_v + K_2 z + C_2 z_v, \\ \dot{z} &= z_v, \\ \dot{z}_v &= u_l, \end{aligned} \tag{5.19}$$

where u_l is the force per unit mass that can be applied on M_2. We get the following equations by taking successive time derivatives of y:

$$\begin{aligned} \dot{y} &= y_v, \\ \ddot{y} &= \frac{-K_{12}y - C_{12}y_v + K_2 z + C_2 z_v}{M_1}, \\ \dddot{y} &= \frac{-K_{12}y_v - C_{12}\dot{y}_v + K_2 z_v + C_2 u_l}{M_1}. \end{aligned} \tag{5.20}$$

From (5.20), one can see that the controller u_l affects $\dddot{y}$ directly. If the right-hand side of $\dddot{y}$ in (5.20) were made to be equal to $\dddot{y}_m - k_1(\ddot{y} - \ddot{y}_m) - k_2(\dot{y} - \dot{y}_m) - k_3(y - y_m)$, corresponding differential equation for error is as follows:

$$\dddot{e} + k_1\ddot{e} + k_2\dot{e} + k_3 e = 0.$$

Therefore, the characteristic polynomial for the error evolution above is:

$$\Delta(s) = s^3 + k_1 s^2 + k_2 s + k_3,$$

where $k_1 > 0$, $k_2 > 0$ and $k_3 > 0$ can be easily found such that $\Delta(s)$ is Hurwitz, which ensures e, $\dot{e}$ and $\ddot{e}$ converge to zero exponentially. Therefore, the control input u_l that ensures $\dddot{y} = \dddot{y}_m - k_1(\ddot{y} - \ddot{y}_m) - k_2(\dot{y} - \dot{y}_m) - k_3(y - y_m)$ in (5.20) may be given as:

$$u_l = \frac{M_1}{C_2}\left[\dddot{y}_m - k_1(\ddot{y} - \ddot{y}_m) - k_2(\dot{y} - \dot{y}_m) - k_3(y - y_m) - F(\dot{y}, y, z, z_v)\right], \tag{5.21}$$

where

$$F(\dot{y}, y, z, z_v) = \frac{1}{M_1^2}\left[-M_1 K_{12}\dot{y} + C_{12}K_{12}y + C_{12}^2\dot{y} - C_{12}K_2 z - C_{12}C_2 z_v + M_1 K_2 z_v\right].$$

For exact tracking, we set $y(t)$ to be identical to $y_m(t)$, for $t \in [0, T]$, in (5.21) to get u_l as follows:

$$u_l = \frac{M_1}{C_2}\left[\dddot{y}_m - F(\dot{y}_m, y_m, z, z_v)\right]. \tag{5.22}$$

Therefore, the estimator for z and z_v is given as follows:

$$\begin{aligned}
\dot{\hat{z}} &= \frac{1}{C_2}[M_1\ddot{y}_m + K_{12}y_m + C_{12}\dot{y}_m - K_2\hat{z}], \\
\dot{\hat{z}}_v &= \hat{u}_l, \\
\hat{z}(0) &= 0, \\
\hat{z}_v(0) &= 0,
\end{aligned} \tag{5.23}$$

where, $\hat{u}_l$ can be obtained by substituting $z = \hat{z}$ and $z_v = \hat{z}_v$ in (5.22). Figure 38 portrays the estimates of z and z_v that are obtained by numerically integrating equation (5.23) for the given initial conditions.

3. Mode detection

The estimates of states $Z = (z_1,\ z_2)$ of the hybrid system (5.8) can be used to determine the mode the system is in at any instant of time $t \in [0, T]$. The mode i $(i = 1,\ 2,\ 3)$ and the time duration Δ_i for that mode may be obtained by determining the time instants for which $|\phi_i(Y_m, \hat{Z}) - u|$ is minimum. For the hybrid system (5.8), $\phi_i(Y_m, \hat{Z})$ $(i = 1,\ 2,\ 3)$ are given as follows:

$$\begin{aligned}
\phi_1(Y_m, \hat{Z}) &= \frac{1}{m}[(y_m - P_{atm})A_b - C_1\hat{z}_2 - K_1\hat{z}_1], \\
\phi_2(Y_m, \hat{Z}) &= \frac{1}{m}[(y_m - P_{atm})A_b - C_2\hat{z}_2 - K_2\hat{z}_1], \\
\phi_3(Y_m, \hat{Z}) &= \frac{1}{m}[(y_m - P_{atm})A_b - C_3\hat{z}_2 - K_3\hat{z}_1],
\end{aligned}$$

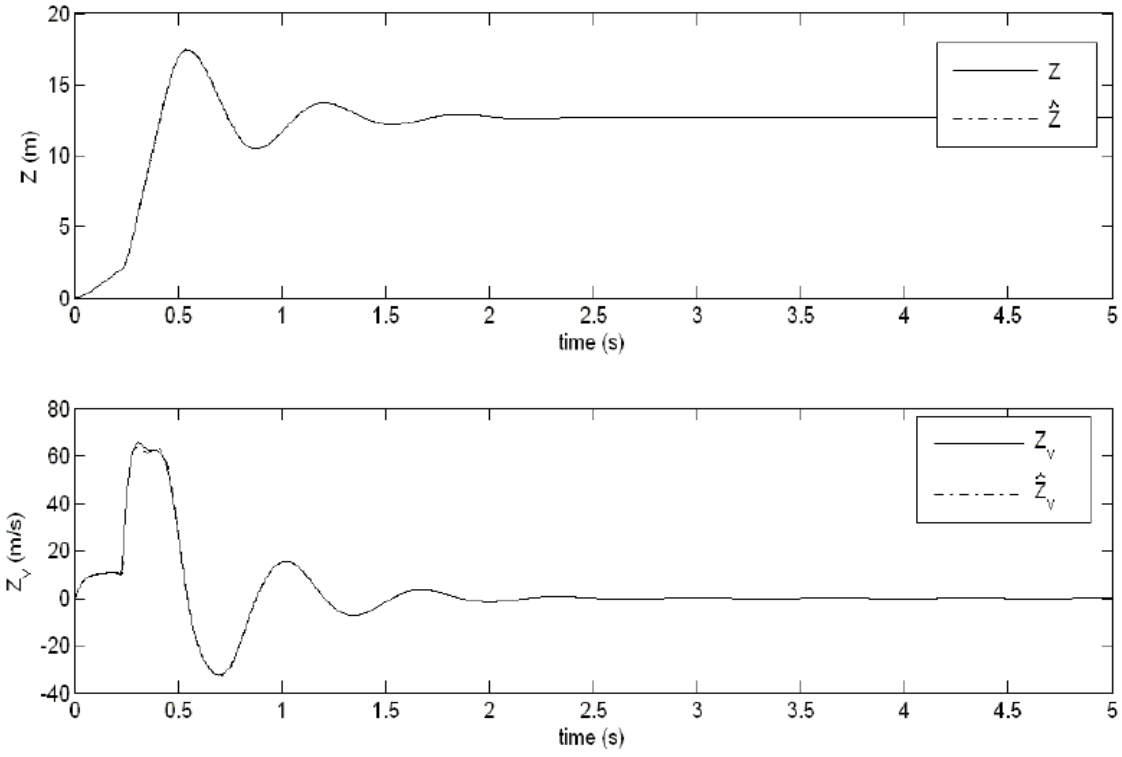

Fig. 38. Steady-state estimates of z and z_v of the mechanical hybrid system

where $\hat{Z} = (\hat{z}_1,\ \hat{z}_2)$ are the system's estimated states and $Y_m = y_m$ is its measured output. The following residuals for each $\phi_i(Y_m, Z)$, over the time interval $[0, T]$, are defined as follows:

$$\begin{aligned} \epsilon_1 &= |\phi_1(Y_m, \hat{Z}) - u|, \\ \epsilon_2 &= |\phi_2(Y_m, \hat{Z}) - u|, \\ \epsilon_3 &= |\phi_3(Y_m, \hat{Z}) - u|, \end{aligned}$$

where $u = u_a$ and is given by (5.16). Therefore, Δ_i is the largest set of continuous sequence of time instants in $[0, T]$ for which the corresponding ϵ_i is minimum. The system is said to be in mode i, atleast, for all $t \in \Delta_i$. Figure 39 shows the modes system (5.8) is in over the time interval $[0, T]$ and the likely time duration for the system in each of these modes.

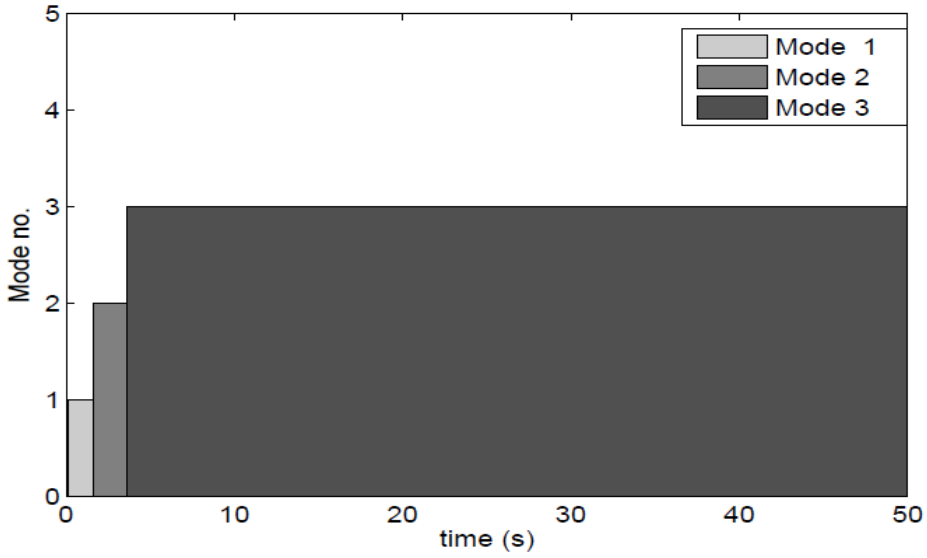

Fig. 39. Mode detection for system (5.8)

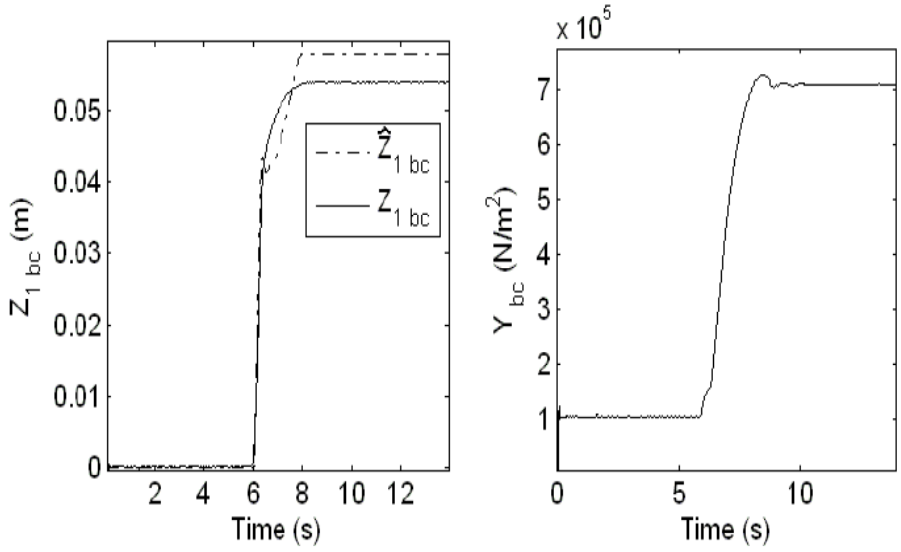

Fig. 40. Pushrod stroke ($z_{1\,bc}(T) = 0.051\ mm$) for "type 20" brake chamber estimated using the scheme

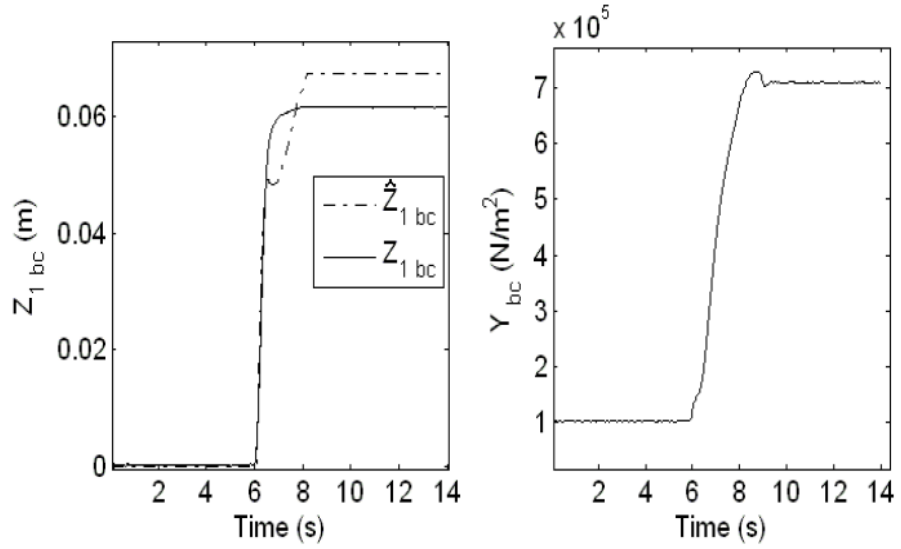

Fig. 41. Pushrod stroke ($z_{1\,bc}(T) = 0.061\ mm$) for "type 30" brake chamber estimated using the scheme

F. Experimental corroboration of the estimation scheme

All the test data obtained are for "full-brake" application wherein the driver of the vehicle fully presses the brake pedal. As a consequence, the metering valve (the treadle valve) remains fully open and the mass flow to the brake chamber stops on when pressure balance is reached across the valve [24]. For this reason, the area of opening (A_p) of the valve was assumed to be constant. Pressure data obtained from the test setup was the output to be tracked and nonlinear system obtained by circumventing the hybrid nature of the air brake system is similar to (5.10). The estimated steady-state pushrod stroke and the measurements from the test setup, for different pushrod strokes, have been compared in Figures 40 and 41.

In general, the area of opening of the metering valve can vary depending on the requirements of the brake system. For example, parameters of the metering valve used in buses may differ from that of those used in trucks due to different load and the kind of load carried by the vehicle. Therefore, the area of openings of the respective valves will differ and it may not be possible to have a universal valve model across all the vehicles. The scheme for steady-state parameter estimation relies on the information about the area of opening of the valve. In absence of this information, an adaptive parameter estimation scheme has been given and corroborated through numerical simulation as well as the test data from the test setup.

G. Problem formulation with parametric uncertainty

As mentioned in the problem formulation with the parameters known, we describe by Y the ordered tuple $(y, y^{(1)}, \ldots, y^{(r-1)})$, by Z the ordered tuple $(z, z^{(1)}, z^{(2)}, \ldots, z^{(l-1)})$ and by θ_j^* $j = 1, \ldots, L$ denote L parameters of the system , so that the governing equations may be described through appropriate smooth functions $f_{10}(Y, Z)$, $f_{00}(Y, Z)$,

$f_{11j}(Y,Z)$, $f_{01j}(Y,Z)$ and possibly a non-smooth function $\phi(Y,Z)$ as:

$$y^{(r)} = f_{10}(Y,Z) + f_{00}(Y,Z)z^{(l)} + \sum_{j=1}^{L} \theta_j^* [f_{11j}(Y,Z) + f_{01j}(Y,Z)z^{(l)}], \quad (5.24)$$

$$z^{(l)} = \phi(Y,Z). \quad (5.25)$$

We will assume that the response of the nonlinear hybrid system (5.24) is stable. The problem is as follows: Suppose $z_1^*, \ldots, z_m^*$ and $\theta_1^*, \theta_2^*, \ldots, \theta_L^*$ are not known. Is it possible to estimate $z(T)$ from the measurement of $y_m(t)$ on the specified interval $[0,T]$? One may assume that the initial conditions are known exactly.

1. Estimation scheme with parametric uncertainty

We follow the procedure similar to the hybrid system with its parameters exactly known. The corresponding nonhybrid system considered is as follows:

$$y^{(r)} = f_{10}(Y,Z) + \sum_{j=1}^{L} \theta_j^* f_{11j}(Y,Z) + \left[f_{00}(Y,Z) + \sum_{j=1}^{L} \theta_j^* f_{01j}(Y,Z) \right] u, \quad (5.26)$$

$$z^{(l)} = u. \quad (5.27)$$

Apart from the assumption that the "internal dynamics" of the system governed by equations (5.24) and (5.25) are stable, we also assume that the term $[f_{00}(Y,Z) + \sum_{j=1}^{L} \theta_j^* f_{01j}(Y,Z)] \neq 0$, so that we may derive a feedback linearizing control law.

Let $k_1, \ldots, k_{r-1}$ be real positive numbers such that the polynomial $\Delta(s) = s^r + k_1 s^{r-1} + \ldots + k_{r-1}$ is Hurwitz, i.e., all the roots of this polynomial have a negative real part. We define an error function $S := e^{(r-1)} + k_1 e^{(r-2)} + \ldots + k_{r-1} e^0$, where $e = y(t) - y_m(t)$. If we choose the evolution equation for S as follows:

$$\dot{S} = -\lambda S, \quad (5.28)$$

where $\lambda > 0$. The error evolution equation is as follows:

$$e^{(r)} + k_1 e^{(r-1)} + \ldots + k_{r-1} e^1 + \lambda(e^{(r-1)} + k_1 e^{(r-2)} + \ldots + k_{r-1} e^0) = 0,$$
$$e^{(r)} + (k_1 + \lambda) e^{(r-1)} + \ldots + (k_{r-1} + \lambda k_{r-2}) e^1 + \lambda k_{r-1} e^0 = 0. \quad (5.29)$$

Also, we can write (5.29) as follows:

$$y^{(r)} = {y_m}^{(r)} - (k_1 + \lambda) e^{(r-1)} - \ldots - (k_{r-1} + \lambda k_{r-2}) e^1 - \lambda k_{r-1} e^0. \quad (5.30)$$

We choose the control law in (5.24) as follows:

$$u = \frac{1}{\left[f_{00}(Y,Z) + \sum_{j=1}^{L} \hat{\theta}_j f_{01j}(Y,Z) \right]} [y_m^{(r)}(t) -$$
$$(k_1 + \lambda)(y^{(r-1)}(t) - y_m^{(r-1)}(t)) - (k_2 + \lambda k_1)(y^{(r-2)}(t) - y_m^{(r-2)}(t))$$
$$- \cdots - \lambda k_{r-1}(y(t) - y_m(t)) - \left[f_{10}(Y,Z) + \sum_{j=1}^{L} \hat{\theta}_j f_{11j}(Y,Z) \right]], \quad (5.31)$$

where $\hat{\theta}_j$ is the estimate of the unknown parameter θ_j^*. We now derive the governing equations for $\hat{\theta}_j$ $j = 1, \ldots, L$.

2. Parameter adaptation law

For the control law given by (5.31), the evolution equation for S reduces to the following:

$$\dot{S} + \lambda S \;=\; \sum_{j=1}^{L} \widetilde{\theta}_j \left[f_{11j}(Y,Z) + f_{01j}(Y,Z) u \right], \quad (5.32)$$

where $\widetilde{\theta}_j = \theta_j^* - \hat{\theta}_j$.

We choose a positive definite function Γ as follows:

$$\Gamma = \frac{S^2}{2} + \left[\sum_{j=1}^{L} \gamma_j \frac{\widetilde{\theta}_j^{\,2}}{2} \right]. \quad (5.33)$$

Therefore, the evolution equation for Γ is as follows:

$$\dot{\Gamma} = -\lambda\frac{S^2}{2} + \left[\sum_{j=1}^{L}\widetilde{\theta}_j\left[f_{11j}(Y,Z) + f_{01j}(Y,Z)u\right]\right]S + \left[\sum_{j=1}^{L}\gamma_j\widetilde{\theta}_j\dot{\hat{\theta}}_j\right], \tag{5.34}$$

where $\gamma_j > 0$. We choose the evolution equation of $\hat{\theta}_j$ as follows:

$$\dot{\hat{\theta}}_j = -\frac{1}{\gamma_j}(f_{11j}(Y,Z) + f_{01j}(Y,Z)u)S. \tag{5.35}$$

Also, the governing equation for $\hat{\theta}_j$, (5.35), ensures that $\dot{\Gamma}$ is negative semi-definite. Then, one may easily see that the control law given by (5.31) and the parameter adaptation law given by (5.35) ensure the desired result for $y(t)$ tracking $y_m(t)$ ([48], [50], [51]):

Hence, we have the following evolution equation for z and $\hat{\theta}_j$ $j = 1, \ldots, L$:

$$\begin{aligned} z^{(l)} &= u, \\ \dot{\hat{\theta}}_j &= -\frac{1}{\gamma_j}(f_{11j}(Y,Z) + f_{01j}(Y,Z)u)S, \end{aligned} \tag{5.36}$$

where u is given by (5.31). Our estimation scheme involves numerically integrating the last equation (5.36) on the interval $[0,T]$. Therefore, Y in the equation (5.36) is known. Since the initial condition for z is assumed known, this equation can be numerically integrated to obtain $z(T)$.

3. Adaptive estimation of A_p

In absence of the exact knowledge of A_p, the controller for the nonlinear system (5.10) will be as follows:

$$u_v = \frac{1}{A_b y}\left[-(\dot{y}_m - k_1(y - y_m))(A_b z_1 + V_{o1}) + \hat{A}_p y\sqrt{2RTlog\left(\frac{P_o}{y}\right)}\right], \tag{5.37}$$

where $\hat{A}_p$ is the estimated area of opening. Therefore, the error $e(t) := y - y_m$ will evolve according to the following differential equation:

$$\dot{e} + k_1 e = \widetilde{A}_p \frac{y\sqrt{2RTlog\left(\frac{P_o}{y}\right)}}{Abz_1 + V_{o1}},$$

where $\widetilde{A}_p = A_p - \hat{A}_p$ and y is the output of (5.10) for u_v given by (5.37). We assume the following form for evolution of the parameter error $\widetilde{A}_p$:

$$\dot{\widetilde{A}}_p = -\gamma e \frac{y\sqrt{2RTlog\left(\frac{P_o}{y}\right)}}{Abz_1 + V_{o1}}.$$

Since the function $w = \frac{y\sqrt{2RTlog\left(\frac{P_o}{y}\right)}}{Abz_1+V_{o1}}$ is bounded over the interval $[0, T]$, it can be shown using *"Barbalat's lemma"*([34], [35]) that the error e will converge to zero (see Appendix C). For the estimated parameter $\hat{A}_p$ to converge to A_p, the function w should be "persistently" exciting([34], [35]) in the interval $[0, T]$. Therefore, the estimators for z_1 and for A_p are as follows:

$$\begin{aligned}
\dot{\hat{z}}_1 &= \frac{1}{A_b y}\left[-(\dot{y}_m - k_1(y - y_m))(A_b\hat{z}_1 + V_{o1}) + \hat{A}_p y\sqrt{2RTlog\left(\frac{P_o}{y}\right)}\right], \\
\dot{\hat{A}}_p &= \gamma(y - y_m)\frac{y\sqrt{2RTlog\left(\frac{P_o}{y}\right)}}{Ab\hat{z}_1 + V_{o1}}, \\
\hat{A}_p(0) &= \hat{A}_{po}, \\
\hat{z}_1(0) &= 0,
\end{aligned} \tag{5.38}$$

where $\hat{A}_{po}$ is some initial guess of the area of opening of the valve. Also y is the output of (5.10) for $\hat{u}_v$ obtained by replacing z_1 by $\hat{z}_1$ in (5.37). Figure 42 shows the estimates of z_1 and A_p obtained by (5.38) for two different values of A_p. Figure 43 shows the estimated steady-state pushrod strokes for different slack adjuster settings.

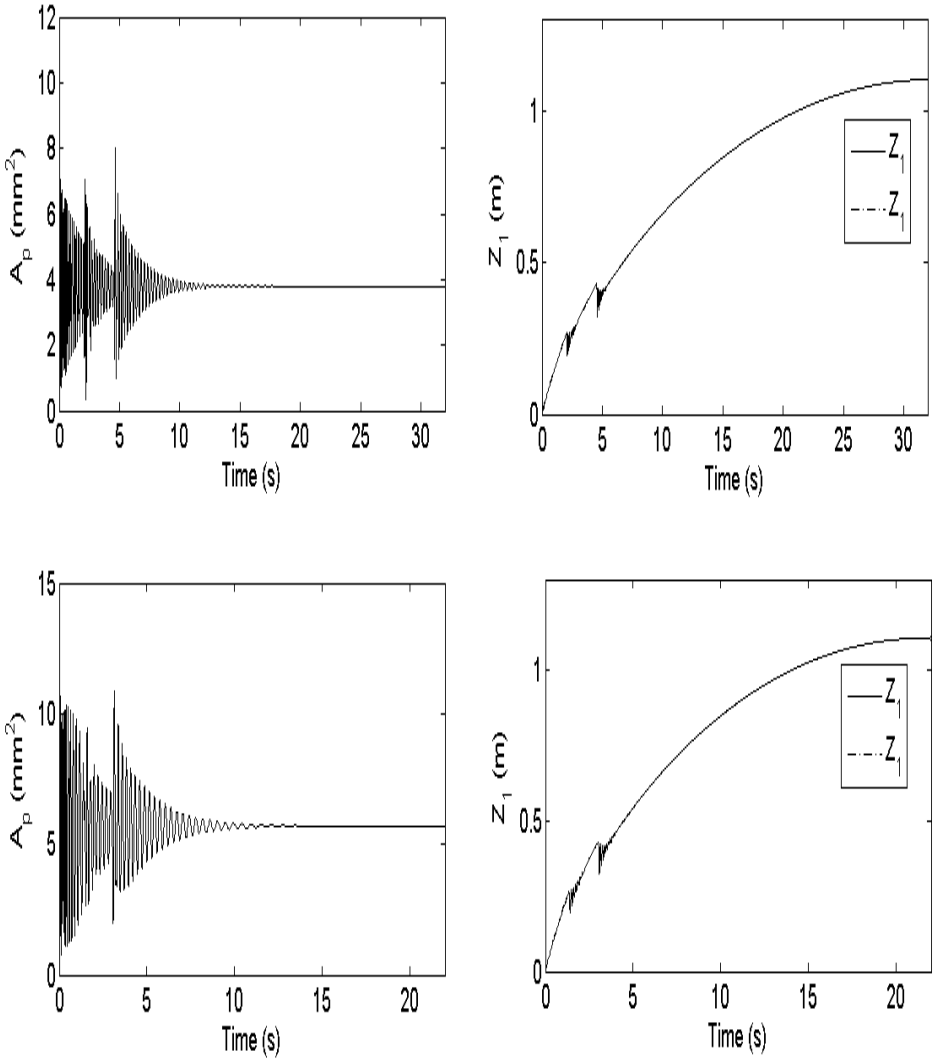

Fig. 42. Steady-state estimate of z_1 and of A_p

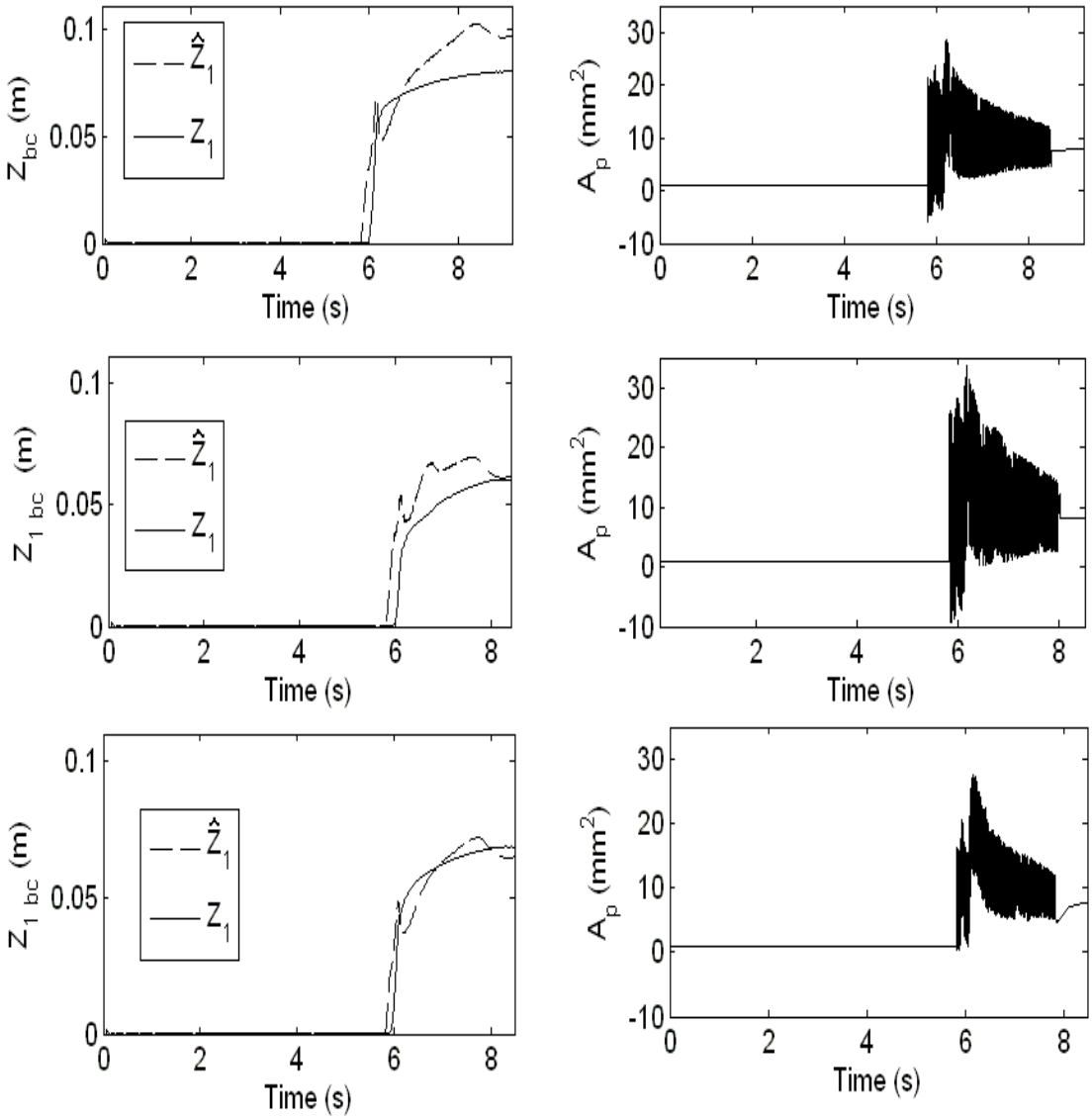

Fig. 43. Pushrod stroke estimates for $z_{1\,bc}(T) \approx 79\ mm,\ 55\ mm,\ 65\ mm$, for rear brake chamber ("type 30") and corresponding estimated area A_p

CHAPTER VI

CONCLUSIONS AND FUTURE SCOPE

In this dissertation, model based diagnostic schemes for the air brake system that estimate the severity of leakage in the system in terms of the mass flow rate of leaking air and estimate the steady-state stroke of the pushrod of the system, have been presented. The diagnostic schemes for leak estimates the severity of the leak based on the look-up table that relates the measured steady-state pressure in the brake chamber to the corresponding leak severity. This look-up table has been developed for the supply pressures of 60 psi, 70 psi, 80 psi and 90 psi. The scheme is expected to predict a presence of those leak severities that elude the standard inspection or do not cause the leak warning systems, present in the vehicle, to get activated.

The scheme for estimation of the steady-state stroke of the pushrod utilizes the measurements of brake chamber pressure and the model for brake chamber energy to predict the steady-state brake chamber energy. From the steady-state estimate of the energy and the measured steady-state pressure, the steady-state volume of the brake chamber is obtained. A functional form for the steady-state volume of the brake chamber that relates the steady-state volume, the area of the brake chamber diaphragm and the steady-state pushrod stroke, has been assumed. This functional form has been used to compute the steady-state pushrod stroke.

The models have been corroborated with the experimental data from the test setup built according to the specifications for the air brake system laid down by Federal Motor Vehicle Safety Standard number 121. The experimental date from the test setup corresponds to the “full-brake” application, a requirement for performing the diagnostics for the brake system, as per the guidelines by Federal Motor Carrier Safety Regulations.

Finally, a parameter estimation technique for "sequential" hybrid systems by circumventing their hybrid nature has been given. The technique indicates that the problem of parameter estimation may be solved by solving the problem of controller design for a modified nonlinear system. This modified system is obtained by disconnecting the part of the hybrid system responsible for its hybrid nature. The controller of the nonlinear system ensures that the output of nonlinear system *"exactly"* tracks the output of hybrid system. The estimates of the parameters of hybrid system are obtained by numerically solving the governing equations for the "internal dynamics" associated with the controlled nonlinear system.

A. Potential impact of the work

The main impact of this dissertation work that has been identified is as follows:

- The scheme for leak is expected to detect and estimate severity of leaks that remain undetected during the inspection process or are not severe enough to activate the warning systems, but are detrimental to the brake system. The leak severity information may be used check if a vehicle is road worthy.

- The scheme estimates the steady state brake chamber energy based on the brake chamber pressure measurements. The steady state pushrod stroke is computed from the estimated steady state energy and the measured steady state chamber pressure. The estimated steady state pushrod stroke may be compared with the out-of-adjustment limits for a given brake chamber (listed in FMVSS 121) which will enable monitoring the out-of-adjustment of air brakes. This information can be used towards development of early warning system for out-of-adjustment.

- Both these scheme can be used to modify existing safety inspection procedures

and develop new inspection tools that can identify the faults, predict their consequence and expedite the inspection.

B. Scope of future work

The following have been identified as the future work that needs to be undertaken towards implementing the developed schemes:

- The most important challenge towards implementing the schemes is the absence of pressure transducers for measuring the brake chamber pressure. A novel way of modifying the existing brake chamber to provide a measurement port for the proposed hand-held device can be exploited and a cost-to-benefit study regarding the modification needs to be undertaken towards its implementation.

- The diagnostic schemes developed in this dissertation are primarily based the look-up table obtained for the leak and the mathematical model for the brake chamber energy of the air brake system. The look-up table has been obtained for Bendix "E-7" treadle valve and for a typical straight truck or a 4×2 tractor configuration of the test setup. In reality, a multitude of combinations of valves and truck / tractor-trailer configurations exist and several full-scale tests need to be performed to verify whether a single look-up table will suffice or not.

- The estimation scheme for pushrod has been corroborated for single brake chamber, brake chambers connected via. separate metering valves (secondary valve and relay valve). The scheme currently assumes that a single brake chamber is connected to the delivery side of a valve. However, in an actual air brake system, more than one brake chambers are connect to the valve's delivery side. The scheme need to be corroborated for a such a configuration.

- Experimental data shows that the leakage of air and the change in pushrod stroke affects the pressure transients of the brake chamber. A "Go-NoGo" pressure curve may be obtained for a brake chamber, which when compared with the measured pressure can be used to quickly determine the road worthiness of the inspected vehicle.

REFERENCES

[1] "National Transportation Statistics 2008," U.S. Department of Transportation Research and Innovative Technology Administration Bureau of Transportation Statistics, Washington, DC, 2008.

[2] "North American Uniform Vehicle Inspection and Out-of-Service Criteria," Commercial Vehicle Safety Alliance, Greenbelt, MD, 1992.

[3] D. Middleton and J. Rowe, " Feasibility of Standardized Diagnostic Device for Maintenance and Inspection of Commercial Motor Vehicles," *Transportation Research Record*, vol. 1560, pp. 48-56, 1996.

[4] "Air Brake System," National Highway Traffic Safety Administration, U.S. Department of Transportation, Washington, DC, Section 571, Standard no. 121.

[5] R.R. Scheibe and P.G. Reinhall, "Safety Monitoring of Air Brake Systems On Board Commercial Vehicles," *Transportation Research Record*, vol. 1560, pp. 40-47, 1996.

[6] "Federal Motor Carrier Safety Regulations: Part 390," National Highway Traffic Safety Administration, U.S. Department of Transportation, Washington, DC, Part.no 390, October 2003.

[7] "2008 Large Truck Crash Overview," Federal Motor Carrier Safety Administration Report-Analysis Division, Publication no. FMCSA-RRA-10-004, U.S. Department of Transportation, Springfield, VA, 2010.

[8] "Report to Congress on the Large Truck Crash Causation Study," Federal Motor Carrier Safety Administration Report, U.S. Department of Transportation, Springfield, VA, November 2005.

[9] "Fatality Investigation Report," Oregon Fatality and Control Evaluation, Center for Research on Occupational and Environmental Toxicology, Oregon Health & Science University, Portland, OR, 2006.

[10] "Safety Recommendation," National Transportation Safety Board, Washington, DC, 1992.

[11] "Safety Recommendation," National Transportation Safety Board, Washington, DC, 2001.

[12] "Revised Costs of Large Truck- and Bus-Involved Crashes," Federal Motor Carrier Safety Administration Report, U.S. Department of Transportation, Springfield, VA, November 2002.

[13] "Highway Special Investigation Report: Selective Motorcoach Issues," National Transportation Safety Board, Washington, DC, 1999.

[14] R. Isermann, "Process Fault Detection Based on Modeling and Estimation Methods - a Survey," *Automatica*, vol. 22, no. 4, pp. 387-404, 1984.

[15] A. Benkherouf and A.Y. Allidina, "Leak Detection and Location in Gas Pipelines," *Control Theory and Applications, IEE Proceedings D*, vol. 135, no. 2, pp. 142-148, 1988.

[16] T. Hsiao and M. Tomizuka, "Observer-based Sensor Fault Detection and Identification with Application to Vehicle Lateral Control," in *Proceedings of the American Control Conference*, 2004, pp. 810-813.

[17] C. Verde, "Minimal Order Nonlinear Observer for Leak Detection," *ASME Journal of Dynamics, Systems, Measurement and Control*, vol. 126, pp. 467-472, 2004.

[18] K. Kannan, I. J. Rao and K. R. Rajagopal, "A thermomechanical framework for the glass transition phenomenon in certain polymers and its application to fiber spinning," *Journal of Rheology*, vol. 46, pp. 977-999, 2002.

[19] S. Dhar, S. Darbha and K.R. Rajagopal, "Identification and Estimation of Parameters Defining a Class of Hybrid Systems," *Nonlinear Analysis: Hybrid Systems*, accepted, 2010.

[20] "How Air Brakes Work," http://auto.howstuffworks.com/auto-parts/brakes/brake-types/air-brake1.htm, accessed June 2009.

[21] G. Westinghouse Jr., "Improvement in Steam-Power-Brake Devices," United States Patent Office, Patent no. 88929, 1869.

[22] L. C. Buckman, *Commercial Vehicle Braking Systems: Air Brakes, ABS and Beyond,* Warrendale, PA: Society of Automotive Engineers Inc., November 1998.

[23] R.J. Morse, "Brake System Performance at Low Operating Pressures," *Society of Automotive Engineers Inc.*, vol. 700512, pp. 1-6, 1970.

[24] "Air Brake Manual by Bendix," http://www.bendixvrc.com/itemDisplay.asp?documentID=5032, accessed May 2008.

[25] *EC Series Electric Cylinders: User's Manual,* PN CUS10050, ver. 1.0, Rockford, IL, Industrial Devices Corp./ Danaher Motion, 1995.

[26] *B8501: Brushless Analog Position Control Manual Supplement*, PN PCW-4712, Rev. 1.01, Rockford, IL, Industrial Devices Corp./ Danaher Motion, 1995.

[27] "Dyla-trol Flow Controls," M.F. Dynamics, http://www.mead-usa.com/products/detail.aspx?id=4, accessed April 2008.

[28] J.C. Gerdes and J.K. Hedrick, "Brake System Modeling for Simulation and Control," *ASME Journal of Dynamics, Systems, Measurement and Control*, vol. 121, pp. 496-503, 1999.

[29] Y.Khan, P.Kulkarni and K.Youcef-Toumi, "Modeling, Experimentation and Simulation of a Brake Apply System," *ASME Journal of Dynamics, Systems, Measurement and Control*, vol. 116, pp. 111-122, 1994.

[30] C.L. Bowlin, S.C. Subramanian, S. Darbha and K.R. Rajagopal, "A Pressure Control Scheme for Air Brakes in Commercial Vehicle," *IEE Journal of Intelligent Transportation Systems*, vol. 153, no. 1, pp. 21-32, 2006.

[31] T. Acarman, U. Ozguner, C. Hatipoglu and A.M. Igusky, "Pneumatic Brake System Modeling for System Analysis," *Transactions of Society of Automobile Engineers*, Paper no. 2000-01-3414, pp. 1-7, 2000.

[32] L.D. Kandt, P.G. Reinhall and R.R. Scheibe, "Determination of Air Brake Adjustment from Air Pressure Data," *Proc. Instn. Mech. Engrs.*, vol. 215, part D, pp. 21-29, 2001.

[33] S.C. Subramanian, S. Darbha and K.R. Rajagopal, "Modeling the Pneumatic Subsystem of an S-cam Air Brake System," *ASME Journal of Dynamics, Systems, Measurement, and Control*, vol. 126, pp. 36-46, 2004.

[34] R.D. Zucker and O. Biblarz, *Fundamentals of Gas Dynamics,* 2nd ed., Hoboken, NJ: John Wiley & Sons Inc., 2002.

[35] M. Saad, *Compressible Fluid Flow,* 2nd ed., Englewood Cliffs, NJ: Prentice-Hall Inc., 1993.

[36] S.C. Subramanian, "A Diagnostic System for Air Brakes in Commercial Vehicles," Ph.D. dissertation, Texas A&M University, College Station, TX, 2006.

[37] R. Srivatsan, S. Dhar, S. Darbha, and K.R. Rajagopal, "Development of a Model for an Air Brake System with Leaks," in *Proceedings of the American Control Conference*, 2009, pp. 1134-1139.

[38] M. Nyberg and A. Perkovic, "Model based diagnosis of leaks in the air-intake system of an SI-engine," *Society of Automotive Engineers spec. publ.*, vol. 1357, pp. 25-31, 1998.

[39] J.L. Crassidis and J.L. Junkins, *Optimal Estimation of Dynamic Systems,* Boca Raton, FL: Chapman & Hall/ CRC, 2004.

[40] University of Sydney, "Aerodynamics for Students," http://www-mdp.eng.cam.ac.uk/library/enginfo/aerothermal_dvd_only/aero/fprops/pipeflow/node22.html, accessed May 2008.

[41] R. Miller, *Flow Measurement Engineering Handbook,* New York: McGraw-Hill Professional, 1996.

[42] B.W. Anderson, *The Analysis and Design of Pneumatic Systems,* New York: John Wiley & Sons, 1967.

[43] "California Commercial Driver's License Manual," http://www.dmv.ca.gov/pubs/cdl_ htm/sec5_ a.htm, accessed June 2009.

[44] D.P. Fuglewicz, "Digital Brake Stroke Sensor," *Advancements in Braking: Analysis, Electrical & Mechanical, Society of Automotive Engineers*, vol. 01, pp. 1-7, 2006.

[45] S.C. Subramanian, S. Darbha and K. R. Rajagopal, "A Diagnostic System for Air Brakes in Commercial Vehicles," *IEEE Transactions on Intelligent Transporation Systems*, vol. 7, pp. 370-376, 2006.

[46] S.V. Natrajan, S.C. Subramanian, S. Darbha and K.R. Rjagopal, "A Model of the Relay Valve used in an Air Brake System," *Nonlinear Analysis: Hybrid Systems*, vol. 1, pp. 430-442, 2007.

[47] S.V. Natrajan, "Modeling the Pneumatic Relay Valve of an S-cam Air Brake System," M.S. thesis, Texas A&M University, College Station, TX, 2005.

[48] S. Sastry, *Nonlinear Systems: analysis, stability and control,* New York: Springer-Verlag, 1999.

[49] H.K. Khalil, *Nonlinear Systems,* 3rd ed., Englewood Cliffs, NJ: Prentice Hall, 2002.

[50] A. Isidori, *Nonlinear Control Systems,* 3rd ed., London, U.K.: Springer-Verlag, 1995.

[51] S. Sastry and A. Isidori, "Adaptive Control of Linearizable Systems," *IEEE Transactions on Automatic Control*, vol. 34, pp. 1123-1131, 1989.

APPENDIX A

CALIBRATION CURVE FOR THE VELOCITY TRANSDUCER

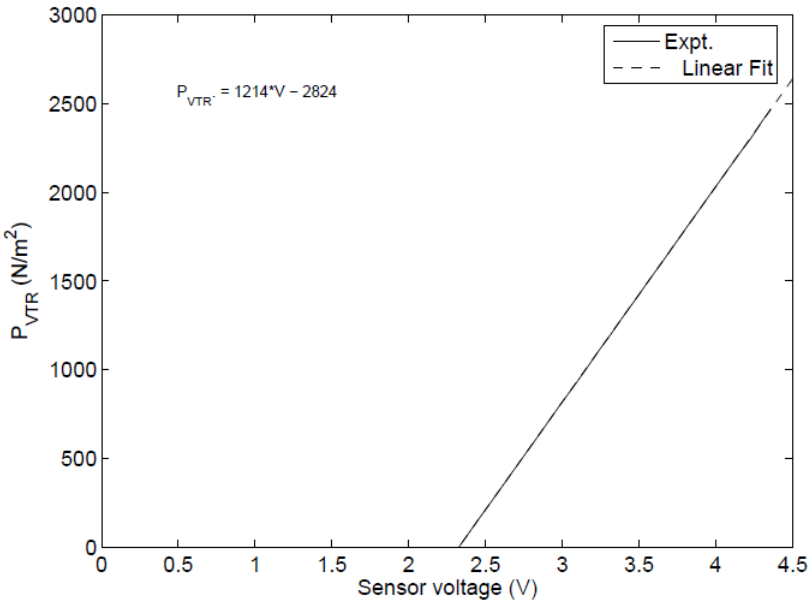

Fig. 44. Calibration curve for the velocity transducer

$$P_{VTR} = 1214V - 2824.$$

where P_{VTR} is the dynamic pressure and is related to the voltage output of the transducer by the equation of the calibration curve above. The centerline velocity of air is compute from P_{VTR} using the following equation:

$$V_{meas} = \sqrt{\frac{2P_{VTR}}{\rho}}.$$

where ρ is the density of air at ambient conditions $\approx 1.22 kg/m^3$.

APPENDIX B

VELOCITY OF FLOW FOR ISOTHERMAL PROCESS

Temperature of air was measured at various points in the test setup during experimentation and varied negligibly during charging of the brake chamber. Therefore, the process has been assumed to be isothermal for the purpose of pushrod stroke estimation. A derivation of velocity of air for isothermal process assumption has been given as follows.

In order to obtain the velocity of flow , we use the balance of linear momentum across the treadle valve:

$$\rho \frac{d\mathbf{v}}{dt} = div\mathbf{T} + \rho\mathbf{b}. \tag{B.1}$$

where $\mathbf{v}$ represents velocity field, $\mathbf{T}$ represents Cauchy stress tensor and $\mathbf{b}$ represents body forces and $\mathbf{b} = 0$, flow in horizontal plane. Also, $\mathbf{T} = -P(\rho)\mathbf{I} = -\rho RT\mathbf{I}$, from ideal gas assumption. In which case, Eq.B.1 modifies as follows:

$$\frac{d\mathbf{v}}{dt} = -RT\text{grad}\rho. \tag{B.2}$$

Taking scalar product with $\mathbf{v}$ on both sides, we get:

$$\mathbf{v}.\frac{d\mathbf{v}}{dt} = -\frac{RT}{\rho}\mathbf{v}.\text{grad}\rho. \tag{B.3}$$

Hence (B.3) modifies as follows:

$$\frac{1}{2}\frac{d\|\mathbf{v}\|^2}{dt} = -\frac{RT}{\rho}\mathbf{v}.\text{grad}\rho. \tag{B.4}$$

Also, the total derivative of density $\rho(x)$ is given by the following:

$$\frac{d\ log\left(\rho(x)\right)}{dt} = \frac{\partial\ log\left(\rho(x)\right)}{\partial t} + \nabla\ log\left(\rho(x)\right).\mathbf{v}. \tag{B.5}$$

Since there is no local change in the density of air w.r.t time, $\frac{\partial log(\rho(x))}{\partial t} = 0$ and $\nabla\ log\left(\rho(x)\right) = \frac{1}{\rho(x)}\text{grad}\rho(x)$. Hence (B.5) reduces to the following:

$$\frac{d\ log\left(\rho(x)\right)}{dt} = \frac{1}{\rho(x)}\text{grad}\rho(x).\mathbf{v}. \tag{B.6}$$

Substituting (B.6) in (B.4), we get the following:

$$\frac{1}{2}\frac{d\|\mathbf{v}\|^2}{dt} = -RT\frac{d\ log\left(\rho(x)\right)}{dt}. \tag{B.7}$$

Integrating (B.7), we get:

$$\|\mathbf{v_1}\|^2 - \|\mathbf{v_2}\|^2 = 2RT\left(log\left(\frac{1}{\rho_1}\right) - log\left(\frac{1}{\rho_2}\right)\right) = 2RTlog\frac{\rho_2}{\rho_1}. \tag{B.8}$$

Here $()_1$ and $()_2$ represent the quantities at the entry and at the exit of the treadle valve. Therefore, the velocity of flow at the exit of the treadle valve (v_2) can be written as:

$$v_2 = \sqrt{{v_1}^2 + 2RTlog\left(\frac{\rho_1}{\rho_2}\right)} \tag{B.9}$$

where v_i is the magnitude of velocity ($\|\mathbf{v_i}\|$) and $v_1 = 0$ (stagnation conditions in the reservoir). Also from the constitutive equation for ideal gas law $P = \rho RT$. Therefore, substituting for ρ, we have the following:

$$v_2 = \sqrt{2RTlog\left(\frac{P_1}{P_2}\right)}. \tag{B.10}$$

APPENDIX C

PROOF OF TRACKING ERROR CONVERGENCE

We can construct a positive definite function W as follows:

$$W = \frac{e^2}{2} + \gamma \frac{\widetilde{A}_p^2}{2}.$$

Therefore $W \geq 0,\ \forall\ t \in [0, \infty)$. Differentiating W, we get:

$$\begin{aligned} \dot{W} &= e\dot{e} + \gamma \dot{\widetilde{A}}_p \widetilde{A}_p, \\ &= -k_1 e^2. \end{aligned}$$

This implies the following:

$$\begin{aligned} W(t) - W(0) &= -k_1 \int_0^t e^2 dt \leq 0, \\ W(t) + k_1 \int_0^t e^2 dt &\leq W(0), \\ \int_0^t e^2 dt &\leq \frac{2W(0)}{k_1}, \\ \lim_{t\to\infty} \int_0^t e^2 dt &\leq \frac{2W(0)}{k_1}. \end{aligned}$$

Therefore, we can say that $\|e\| \leq \sqrt{\frac{2W(0)}{k_1}}$ is bounded $\ \forall\ t \in [0, \infty)$. Also, $W(t) \leq 2W(0) \ \Rightarrow\ \|\widetilde{A}_p\| \leq \sqrt{\frac{2W(0)}{\gamma}}$, hence bounded. Differentiating $\dot{W}$, we get the following:

$$\begin{aligned} \ddot{W} &= -k_1 \dot{e} e, \\ &= -k_1 e^2 - k_1 e \widetilde{A}_p \frac{y\sqrt{2RTlog\left(\frac{P_o}{y}\right)}}{Abz_1 + V_{o1}}. \end{aligned}$$

This implies $\ddot{W}$ is bounded and from Barbalat's lemma, $\dot{W} \to 0 \Rightarrow e \to 0$ as $t \to \infty$.

VITA

Sandeep Dhar was born in Anantnag, a town in the state of Jammu & Kashmir, India. He joined University of Mumbai, India in 1999 and graduated in 2003 with the degree of B. E. in mechanical engineering. He decided to pursue graduate studies and joined Indian Institute of Technology Bombay, Mumbai, India in 2003 and graduated with the degree of Master of Technology in mechanical engineering in 2006. He joined Texas A&M University in 2006 and received his Ph.D. in mechanical engineering in 2010. He may be contacted through:

Dr. Swaroop Darbha

Professor

Department of Mechanical Engineering

Texas A&M University

College Station, Texas, USA, 77843-3123.

or

e-mail: deepu131981@gmail.com.

This document was typeset in LaTeX by Sandeep Dhar.